2

AEFA Project No. 87-08

AEFA

PRELIMINARY AIRWORTHINESS EVALUATION OF MODIFIED SECOND-GENERATION PNEUMATIC BOOT DEICING SYSTEM ON A JUH-1H

James D. Brown
MAJ, AV
Project Officer/Pilot

Charles E. Cassil
Project Engineer

Michael K. Herbst
Project Engineer

October 1988

Final Report

Approved for public release, distribution unlimited.

AVIATION ENGINEERING FLIGHT ACTIVITY
Edwards Air Force Base, California 93523-5000

DISCLAIMER NOTICE

The findings of this report are not to be construed as an official Department of the Army position unless so designated by other authorized documents.

DISPOSITION INSTRUCTIONS

Destroy this report when it is no longer needed. Do not return it to the originator.

TRADE NAMES

The use of trade names in this report does not constitute an official endorsement or approval of the use of the commercial hardware and software.

UNCLASSIFIED
SECURITY CLASSIFICATION OF THIS PAGE

REPORT DOCUMENTATION PAGE

Form Approved OMB No. 0704-0188

1a. REPORT SECURITY CLASSIFICATION UNCLASSIFIED	1b. RESTRICTIVE MARKINGS
2a. SECURITY CLASSIFICATION AUTHORITY U.S. ARMY AVIATION SYSTEMS COMMAND	3. DISTRIBUTION/AVAILABILITY OF REPORT
2b. DECLASSIFICATION/DOWNGRADING SCHEDULE	
4. PERFORMING ORGANIZATION REPORT NUMBER(S) AEFA PROJECT NO. 87-08	5. MONITORING ORGANIZATION REPORT NUMBER(S)
6a. NAME OF PERFORMING ORGANIZATION U.S. ARMY AVIATION ENGINEERING FLIGHT ACTIVITY 6b. OFFICE SYMBOL (If applicable)	7a. NAME OF MONITORING ORGANIZATION
6c. ADDRESS (City, State, and ZIP Code) EDWARDS AIR FORCE BASE, CALIFORNIA 93523-5000	7b. ADDRESS (City, State, and ZIP Code)
8a. NAME OF FUNDING/SPONSORING ORGANIZATION U.S. ARMY AVIATION SYSTEMS COMMAND 8b. OFFICE SYMBOL (If applicable)	9. PROCUREMENT INSTRUMENT IDENTIFICATION NUMBER
8c. ADDRESS (City, State, and ZIP Code) 4300 GOODFELLOW BLVD. ST. LOUIS, MO 63120-1798	10. SOURCE OF FUNDING NUMBERS PROGRAM ELEMENT NO.: EK8-PW827E PROJECT NO.: KEC TASK NO: WORK UNIT ACCESSION NO:

11. TITLE (Include Security Classification)
PRELIMINARY AIRWORTHINESS EVALUATION OF MODIFIED SECOND-GENERATION PNEUMATIC BOOT DEICING SYSTEM ON A JUH-1H

12. PERSONAL AUTHOR(S)
MAJ James D. Brown, Charles E. Cassil, Michael K. Herbst

13a. TYPE OF REPORT	13b. TIME COVERED	14. DATE OF REPORT (Year, Month, Day)	15. PAGE COUNT
FINAL	FROM 26/10/87 TO 7/04/88	OCTOBER 1988	62

16. SUPPLEMENTARY NOTATION

17. COSATI CODES		
FIELD	GROUP	SUB-GROUP

18. SUBJECT TERMS (Continue on reverse if necessary and identify by block number)
Endurance Limit, Handling Qualities, Level Flight Performance, Pitch Link Load, PBDS Activation During Level Flight, ~~Modified Second-Generation Pneumatic Boot Deicing System~~, Structural Loads

19. ABSTRACT (Continue on reverse if necessary and identify by block number)

The U.S. Army Aviation Engineering Flight Activity conducted a Preliminary Airworthiness Evaluation of a modified second-generation Pneumatic Boot Deicing System (PBDS) on a JUH-1H helicopter ~~between 26 October 1987 and 7 April 1988~~. This consisted of a structural loads survey, level flight performance evaluation, and a qualitative handling qualities evaluation. ~~This~~ evaluation was conducted at Edwards Air Force Base, California ~~and Bakersfield, California~~. Twelve flights were conducted for a total of 7.8 productive flight hours. Rotor system structural loads were generally lower than those reported for the unmodified second-generation PBDS. With the PBDS inflated, main rotor pitch link load reached the endurance limit at [illegible] knots indicated airspeed in level flight.. Power required in level flight was less than or equal to power required by the unmodified second-generation PBDS. Inflating the PBDS generated moderate right yaw rates and engine torque rises as great as eight pounds per square inch. One previously identified shortcoming, the aircraft response to PBDS activation during level flight, still exists.

20. DISTRIBUTION/AVAILABILITY OF ABSTRACT ☐ UNCLASSIFIED/UNLIMITED ☒ SAME AS RPT. ☐ DTIC USERS	21. ABSTRACT SECURITY CLASSIFICATION UNCLASSIFIED	
22a. NAME OF RESPONSIBLE INDIVIDUAL SHEILA R. LEWIS	22b. TELEPHONE (Include Area Code) (805) 277-2115	22c. OFFICE SYMBOL SAVTE-PR

DD Form 1473, JUN 86 Previous editions are obsolete.

SECURITY CLASSIFICATION OF THIS PAGE
UNCLASSIFIED

TABLE OF CONTENTS

PAGE

INTRODUCTION

BACKGROUND

1. The Pneumatic Boot Deicing System (PBDS) for the UH-1H helicopter consists of a leading edge cuff on each main rotor blade which is inflatable by engine bleed air. The system was designed by B.F. Goodrich Company (BFG). Tests of two developmental versions of the PBDS were conducted by the U.S. Army Aviation Engineering Flight Activity (AEFA) (refs 1 and 2, app A). The third-generation design was shown in previous testing (ref 2) to generate unacceptable loads in the flight control system during forward flight. In addition, erosion on the second-generation system was unacceptable. Under the current program, modifications to the second- and third-generation systems were to be made by BFG in an attempt to alleviate these problems. In April 1987, the U.S. Army Aviation Systems Command requested that AEFA conduct a Preliminary Airworthiness Evaluation (PAE) of the modified second- and third-generation PBDS. The modified third-generation PBDS was not fabricated and therefore not tested.

TEST OBJECTIVES

2. The objectives of this PAE were to conduct a qualitative evaluation of the handling qualities of the UH-1H with the modified second-generation PBDS and to determine any load or performance differences between the second-generation PBDS and the modified second-generation PBDS on the UH-1H helicopter.

DESCRIPTION

3. The UH-1H is a thirteen-place, single-engine helicopter with a single two-bladed teetering main rotor and a two-bladed tail rotor. The maximum gross weight is 9500 pounds. Power is provided by a Lycoming T53-L-13B free turbine engine rated at 1400 shaft horsepower (shp) uninstalled at sea level standard day conditions. The main transmission is limited to 1137 shp for continuous operation. A more detailed description of the UH-1H is contained in reference 3. The aircraft used in this evaluation, USA S/N 70-16318, is a production UH-1H modified to incorporate a partial ice protection system (Kit A) (described in ref 4), a rotor brake, and the PBDS.

4. The PBDS consists of a prototype ESTANE® deice boot installed on the leading edge of a standard UH-1H rotor blade and is intended to remove accumulated ice through pneumatic expansion (inflation) of chordwise and spanwise tubes. The PBDS also includes a modified main rotor mast, electrical and pneumatic sliprings, associated controllers, electrical components, and air supply components for providing engine bleed air to the PBDS. Customer bleed air from the engine is routed to the deicers in a single inflation activation cycle. A normal activation cycle consists of inflation of the deicer boots for approximately two seconds, followed by deflation. The modified second-generation pneumatic boot is designed to improve erosion resistance and reduce installation drag without compromising ice protection (ref 5). The modification consisted of removing the existing deicer/erosion materials from the outboard 41 inches (station 247.0 to station 288.0) of the rotor blade. The blade leading edge surface from station 273.0 to station 288.0 (15 inches) was restored to the bare surface condition. The

existing deicer/erosion materials between the end of the 15-inch bare blade section and station 247.0 were replaced with a .175-inch thick erosion material with a leading edge radius that matches that of the bare blade. These modifications are shown in figures 1 and 2. A more detailed description of the nonstandard features of the test aircraft, the pneumatic deicing boots, and the boot modifications is contained in appendix B and in reference 5.

TEST SCOPE

5. The PBDS evaluation consisted of a flight loads survey and level flight performance and qualitative handling qualities tests of the UH-1H with the modified second-generation PBDS installed and operational. Testing was conducted at Edwards Air Force Base, California and Bakersfield, California between 26 October 1987 and 7 April 1988. The evaluation required a total of 20.3 flight hours, of which 7.8 hours were productive. BFG provided and installed the pneumatic boot system on the main rotor blades. The test aircraft was operated within the limitations of the operator's manual (ref 3) as amended by the airworthiness release (ref 6). Flight tests were conducted at the conditions shown in tables 1 and 2.

TEST METHODOLOGY

6. Established flight test techniques (ref 7) were used whenever possible throughout this evaluation. Test methods used are briefly discussed in the Results and Discussion section of this report . The Handling Qualities Rating Scale (HQRS) (fig. D-1) was used to supplement the pilot's qualitative comments. Flight test data was recorded manually and by onboard magnetic tape. Loads data were monitored real-time via telemetry (TM) during loads testing. A detailed listing of test instrumentation is contained in appendix C. Data analysis methods are presented in appendix D.

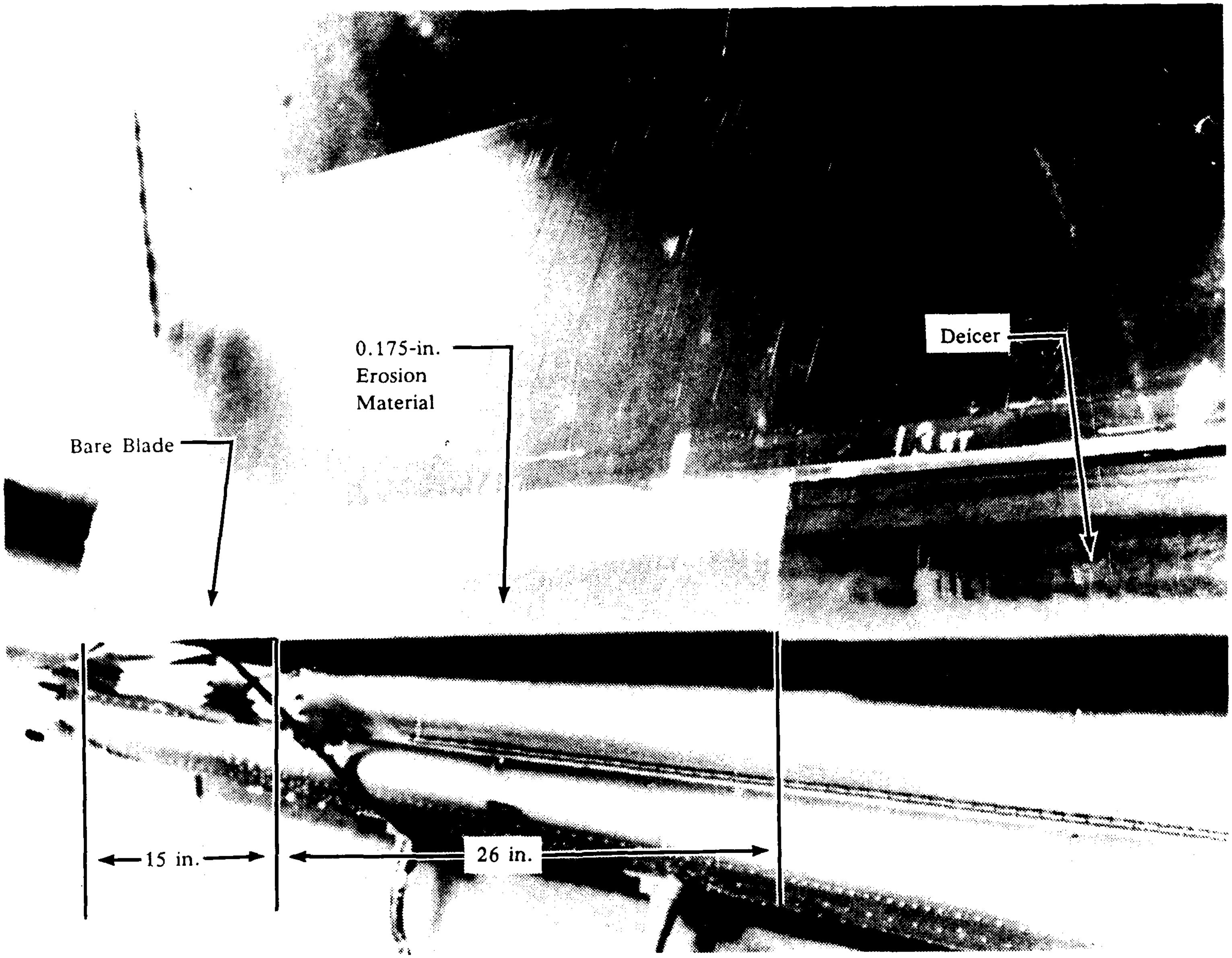

Figure 1. Modified Second-Generation PBDS - View Looking Down at Leading Edge

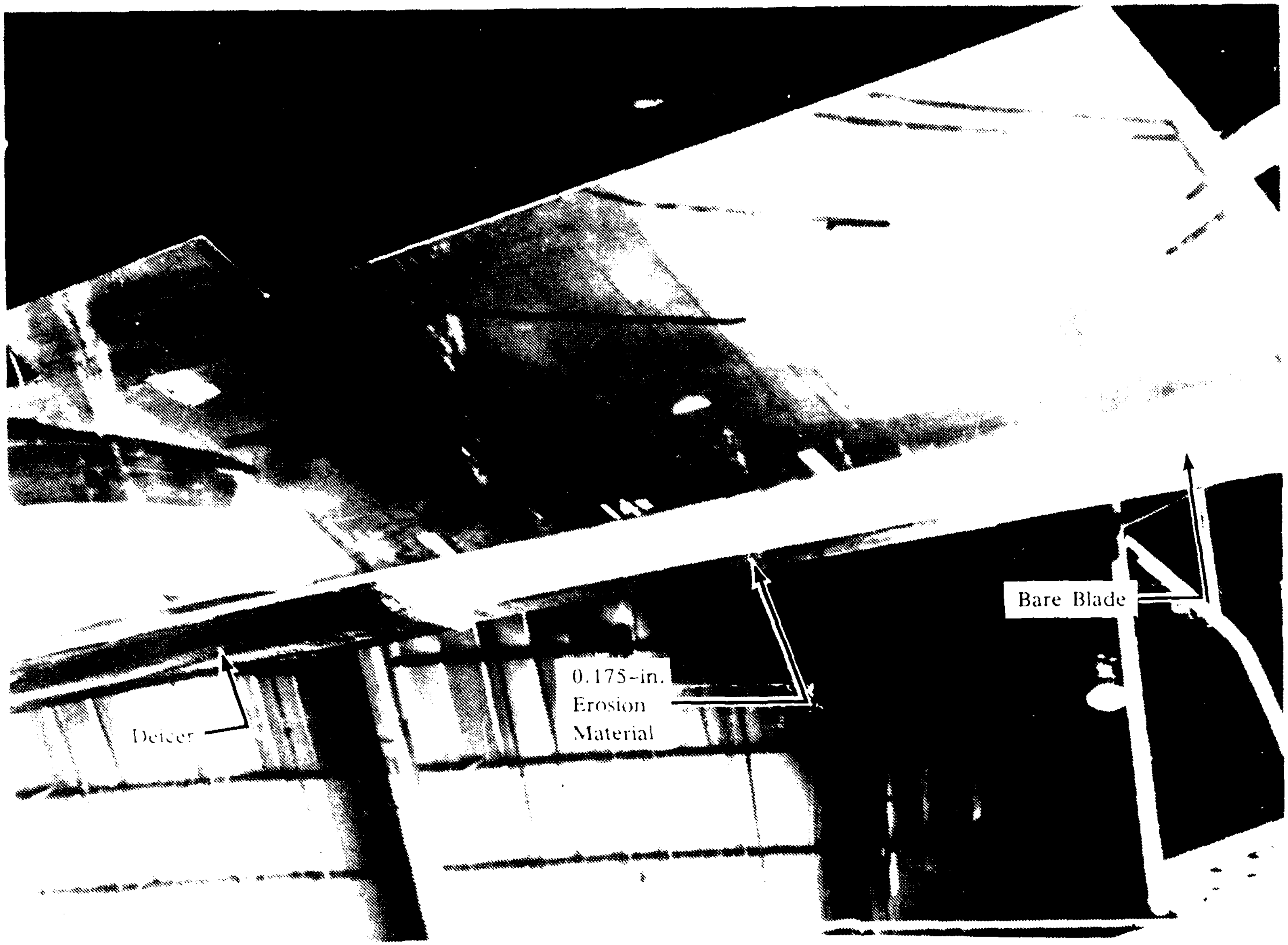

Figure 2. Modified Second-Generation PBDS – View Looking Up at Blade Trailing Edge

Table 1. Loads Survey Test Conditions[1]

Test	Average Gross Weight (lb)	Average Density Altitude (ft)	Average Calibrated Airspeed (kt)	Rotor Speed (rpm)	Pneumatic Boot Configuration	Remarks
Hover	7790	2290	0	324	Deflated Inflated Vented	
Low-Speed Flight	7580-7780	2020-2440	10 and 20 KTAS[2]	321		0-, 90-, 180-, and 270-deg azimuths
	7610	1770	40 KTAS	323	Deflated Inflated	0-deg azimuth
Level Flight	7350-7430	6600-6830	60-112	310	Deflated Inflated Vented	
	7370-7590	5380-6820	58-112	321		
	7330	6760	121	311	Deflated Vented	
	7460	6560	120	321		
Climb	7440	7010	73	320	Deflated Inflated Vented	Torque pressure = 45 psi[3]
	7430	6640	100	321		
Descent	7440	Data not available	70	323		Torque pressure = 8 psi
	7430	6590	100	322		
Autorotation	7640	6760	80	313	Vented	
Right Turn	7070	6060[4]	101	322	Deflated Inflated Vented	30-deg bank
Left Turn	7060	6180[4]	99	322		
Simulated Engine Failure	7030	6180[4]	70	324	Vented	
	7020		100	324		

NOTES:

[1]Utility configuration, mid center of gravity.
[2]KTAS: Knots true airspeed.
[3]psi: Pounds per square inch.
[4]Approximate density altitude at start of test.

Table 2. Level Flight Performance Test Conditions[1]

Average Gross Weight (lb)	Average Longitudinal Center of Gravity (FS)	Average Density Altitude (ft)	Trim True Airspeed (kt)	Average Referred Rotor Speed (rpm)	Pneumatic Boot Configuration
7520	136.1	5,550	40 to 115	319.8	Deflated
8020	133.3	7,100	41 to 123		
8200	133.6	11,420	45 to 105	319.9	
7750	132.4	8,190	43 to 127		Vented

NOTE:

[1]Utility configuration, mid center of gravity, level, zero-sideslip, unaccelerated flight.

RESULTS AND DISCUSSION

GENERAL

7. The structural loads survey tests of the JUH-1H with the modified second-generation Pneumatic Boot Deicing System (PBDS) were conducted at gross weights of approximately 7000 pounds to 7800 pounds and at density altitudes of approximately 1800 feet to 7000 feet. The loads survey tests were conducted with the modified second-generation PBDS in three configurations: (1) deflated, (2) inflated, and (3) vented. Rotor system loads were generally lower than loads reported for the unmodified second-generation PBDS. The main rotor pitch link load reached the endurance limit with the PBDS installed at 100 knots indicated airspeed (KIAS) in level flight at a main rotor speed of 321 rpm, and was within 10 percent of the endurance limit at 90 KIAS in a right turn at a 30-degree bank angle. At all other test conditions, rotor system loads were below endurance limits. Power required by the modified second-generation PBDS in level flight was less than or equal to power required by the unmodified second-generation PBDS. Inflating the PBDS generated a moderate right yaw rate and engine torque pressure rises as great as eight pounds per square inch (psi). The aircraft response to PBDS activation during level flight is a previously identified shortcoming.

STRUCTURAL LOADS SURVEY

8. Loads survey tests were conducted on the modified second-generation PBDS to establish an operational envelope for further testing and were evaluated at the test conditions listed in table 1. Data are presented in tables E-1 through E-4, appendix E.

9. For test purposes, three blade deicer configurations were used: (1) deflated with vacuum (normal configuration), (2) inflated, representing the pneumatically expanded boot condition reached immediately after PBDS activation (a PBDS activation cycle is a single inflation followed immediately by deflation), and (3) vented, representing a failure mode caused by loss of engine bleed air allowing the boots to inflate partially.

10. The pitch link axial loads were well below the limit with the PBDS in the normal deflated condition at airspeeds up to 110 KIAS at 314 and 324 rpm. Activation of the PBDS resulted in an increase in oscillatory loads. At an airspeed of 100 KIAS in level flight, the pitch link axial oscillatory load reached the endurance limit during PBDS activation. The system was not activated at airspeeds above 100 KIAS. Activation of PBDS in a right turn (30-degree bank angle) at 90 KIAS produced a pitch link axial oscillatory load within 10 percent of the endurance limit. In general, loads experienced during this test were lower than loads reported for the second-generation PBDS (ref 2, app A). The following restrictions to the flight envelope of the UH-1 equipped with the modified second-generation PBDS should be observed because of the main rotor pitch link loads experienced during this evaluation:

a. Do not activate the PBDS at airspeeds greater than 90 KIAS.

b. Do not activate the PBDS during turning flight.

LEVEL FLIGHT PERFORMANCE

11. Level flight performance of the JUH-1H with the modified second-generation PBDS installed was evaluated in zero-sideslip level flight using the constant gross weight to ambient pressure ratio (W/δ) method. The evaluation was performed at the conditions of table 2. Results for the deflated PBDS are presented in figures E-1 through E-5. Nondimensional level flight performance data for the deflated PBDS is plotted with nondimensional level flight performance curves for standard blades and unmodified second-generation PBDS for advance ratios (μ's) of 0.10 through 0.22 in figures E-6 through E-12. Results for the vented PBDS are presented in figure E-13. As shown by figures E-6 through E-12, the trend of power coefficient (C_P) versus thrust coefficient (C_T) for the modified second-generation PBDS was different from the trends of C_P versus C_T for both the standard blade and the unmodified second-generation PBDS at each value of μ. Because of this, the level flight performance evaluation of the modified second-generation PBDS was repeated at C_T's of approximately 0.0032 and 0.0043. The results of these repeated evaluations were not significantly different than the results of the initial evaluation. The power required by the modified second-generation PBDS was less than or equal to the power required by the unmodified second-generation PBDS at all conditions tested.

HANDLING QUALITIES

12. Handling qualities of the JUH-1H with the modified second-generation PBDS were qualitatively evaluated in conjunction with the loads survey and performance testing at the conditions of tables 1 and 2. Handling qualities of the JUH-1H with the modified second-generation PBDS in the deflated and vented configurations were essentially unchanged from those of the standard UH-1H. The response of the JUH-1H to activation of the PBDS was evaluated during hover and level flight. Activation of the PBDS system generated moderate right yaw rates and engine torque pressure rises as great as eight psi.

13. Activation of the PBDS at a hover with controls fixed caused a moderate right yaw rate, a slight right roll, and a slight climb. With the pilot in the control loop during PBDS activation, precise control of aircraft attitudes could be accomplished, but required inputs to all controls.

14. Activation of the PBDS during level flight at 80 KIAS with controls fixed caused an immediate right roll to 20-degree bank angle and a 5-degree nose-down change in pitch attitude. Approximately four seconds after activation the bank angle increased to 30 degrees. Maintaining heading within five degrees and airspeed within five knots during activation of the PBDS during level flight at 80 KIAS required an immediate 1/4- to 1/2-inch left directional control input and 1/4-inch aft longitudinal and left lateral cyclic inputs (HQRS 4). The aircraft response to PBDS activation during level flight is a previously reported shortcoming and should be corrected in future PBDS designs.

15. The following **CAUTIONS** should be included in the airworthiness releases for UH-1H's equipped with the PBDS system because of the aircraft handling qualities and engine torque rises during PBDS activation:

CAUTION

When activating the PBDS, moderate right yaw rates can be generated.

CAUTION

When activating the PBDS, torque pressure rises as great as eight psi can occur, which can result in an engine overtorque.

CONCLUSIONS

GENERAL

16. With the modified second-generation Pneumatic Boot Deicing System (PBDS) installed, main rotor system loads are below endurance limits for most flight conditions evaluated and, in general, are lower than loads with the unmodified second-generation PBDS (para 10).

17. The trend of power coefficient (C_P) versus thrust coefficient (C_T) for the modified second-generation PBDS was different from the trends of C_P versus C_T for both the standard blade and the unmodified second-generation PBDS (para 11).

18. The power required by the modified second-generation PBDS was less than or equal to the power required by the unmodified second-generation PBDS (para 11).

19. Handling qualities of the JUH-1H with the modified second-generation PBDS in the deflated and vented configurations are essentially unchanged from those of the standard UH-1H (para 12).

SPECIFIC

20. Main rotor pitch link axial oscillatory load reaches the endurance limit during PBDS activation at 100 knots indicated airspeed (KIAS) in level flight (para 10).

21. Main rotor pitch link axial oscillatory load reaches 90 percent of the endurance limit during PBDS activation at 90 KIAS in a right turn at a 30-degree bank angle (para 10).

SHORTCOMING

22. The aircraft response to PBDS activation during level flight is a previously reported shortcoming (para 14).

RECOMMENDATIONS

23. The following recommendations are made.

a. The shortcoming identified in paragraph 22 should be corrected in future Pneumatic Boot Deicing System (PBDS) designs (para 14).

b. The following restrictions should be made to the flight envelope of the UH-1 equipped with the modified second-generation PBDS (para 10):

(1) Do not activate the PBDS at airspeeds greater than 90 KIAS.

(2) Do not activate the PBDS during turning flight.

c. The following **CAUTIONS** should be included in the airworthiness releases for UH-1H equipped with the PBDS (para 15):

CAUTION

When activating the PBDS, moderate right yaw rates can be generated.

CAUTION

When activating the PBDS, torque pressure rises as great as eight psi can occur, which can result in an engine overtorque.

APPENDIX A. REFERENCES

1. Final Report, AEFA Project No. 81-11, *JUH-1H Pneumatic Boot Deicing System Flight Test Evaluation*, May 1983.

2. Final Report,, AEFA Project No. 83-13, *JUH-1H Redesigned Pneumatic Boot Deicing System Flight Test Evaluation*, August 1987.

3. Technical Manual, TM 55-1520-210-10, *Operator's Manual UH-1H/V Helicopters*, 1 December 1986.

4. Supplement to Technical Manual, TM 55-1520-210-10, *Operator's Manual, UH-1H Helicopter, Serial No. 70-16318, Incorporating an Advance Ice Protection System and UH-1H Kit A Ice Protection*, 19 July 1978.

5. B.G. Goodrich Company, Report No. 87-32-015, *Plan for Aerodynamic Drag Reduction/Erosion Evaluation UH-1H Rotor Blade Pneumatic Deicer System*, 20 February 1987.

6. Letter, AVSCOM, AMSAV-E, 28 November 1983, last revised 8 October 1987 (revision 6), subject: Experimental Airworthiness Release for JUH-1H S/N 70-16318 with Main Rotor Pneumatic Boot Deicing System (PBDS), Main Rotor Brake, and Advanced Icing Severity Level Indicating System Installed.

7. Engineering Design Handbook, Army Materiel Command, AMC Pamphlet 706-204, *Helicopter Performance Testing*, 1 August 1975.

APPENDIX B. DESCRIPTION

1. The test aircraft, USA S/N 70-16318, is a JUH-1H helicopter which incorporates ice protection for the pitot-static tube and the engine air inlet. The Pneumatic Boot Deicing System (PBDS) was installed to provide protection for the main rotor blades. A partial ice protection system (Kit A) provided protection for both the pilot's and copilot's windshields during the structural loads survey. After the completion of the loads survey and before the start of the level flight performance evaluation, the copilot's windshield cracked and was replaced with a standard (unheated) windshield. The level flight performance evaluation was performed with a standard copilot's windshield installed in the helicopter. Nonstandard features of the test helicopter are the PBDS, ice detectors, and Kit A. The PBDS consists of a prototype ESTANE® deice boot, as shown in figure B-1, installed on the leading edge of a standard UH-1H rotor blade which is intended to remove accumulated ice through pneumatic expansion (inflation) of chordwise and spanwise tubes. The PBDS also includes a modified main rotor mast, electrical and pneumatic sliprings, associated controllers, electrical components, and air supply components for providing engine bleed air to the PBDS, as shown in figure B-2. The PBDS installation consists of six major components: the PBDS regulator-reliever/shut-off valve, ejector flow control valve, timer, rotary union, hose and flap assembly, and the pneumatic deicer. PBDS and Kit A component locations are shown in figures B-3 and B-4.

2. Customer bleed air from the engine is routed through a check valve to the regulator-reliever/shut-off valve, which is manually adjusted to the system operating pressure of 25 pounds per square inch (psi). The solenoid-operated ejector flow control valve (electrically energized by the timer) directs bleed air through the pneumatic rotary union to the deicers in a single inflation activation cycle. A normal activation cycle consists of inflation of the deicer boots for approximately two seconds, followed by deflation. With the solenoid deenergized, the ejector flow control valve provides the vacuum necessary to keep the deicers deflated by directing bleed air overboard. A shop air test connection is installed downstream of the checkvalve for leak and maintenance checks. An electrical/manual gate valve is provided upstream of the rotary union to capture pressure or vacuum in the deicer boots and prevent deflation during performance testing or leak checks. The pressure gauge downstream of the regulator-reliever/shut-off valve displays regulated pressure of the ejector control valve. A vacuum/pressure gauge downstream of the gate valve displays the vacuum or pressure of the deicer boots. To evaluate a degraded mode that would occur with engine failure or damage to the PBDS, vacuum to the deicer boots can be removed by use of the regulator-reliever/shut-off valve. This allows the deicer boots to vent to ambient atmospheric conditions through the deenergized ejector control valve, resulting in partial boot inflation (auto-inflation) from different air pressures and centrifugal forces on the rotor blades.

3. The check valve is a basic axial flow, spring-loaded, poppet type unit. During normal operation, the valve poppet is open and has low resistance to flow of air from the engine compressor bleed air supply connection. The valve is designed to prevent air flow leakage into the engine during ground tests of the PBDS.

4. The regulator portion is a single-stage, diaphragm-type unit. When the regulated pressure reaches the regulator set point, the pressure on a diaphragm closes a port,

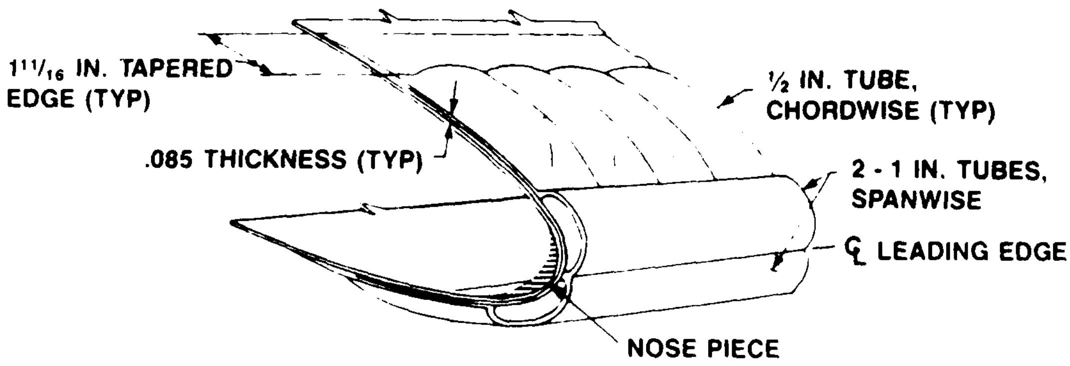

Figure B-1. Typical Cross Section of Installed Deicer Boot (Inflated)

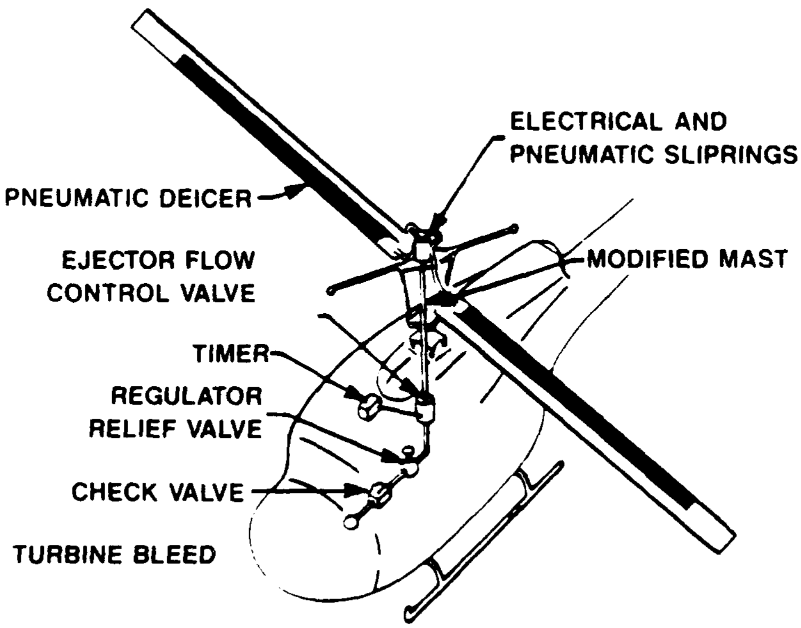

Figure B-2. Pneumatic Deicer System Components

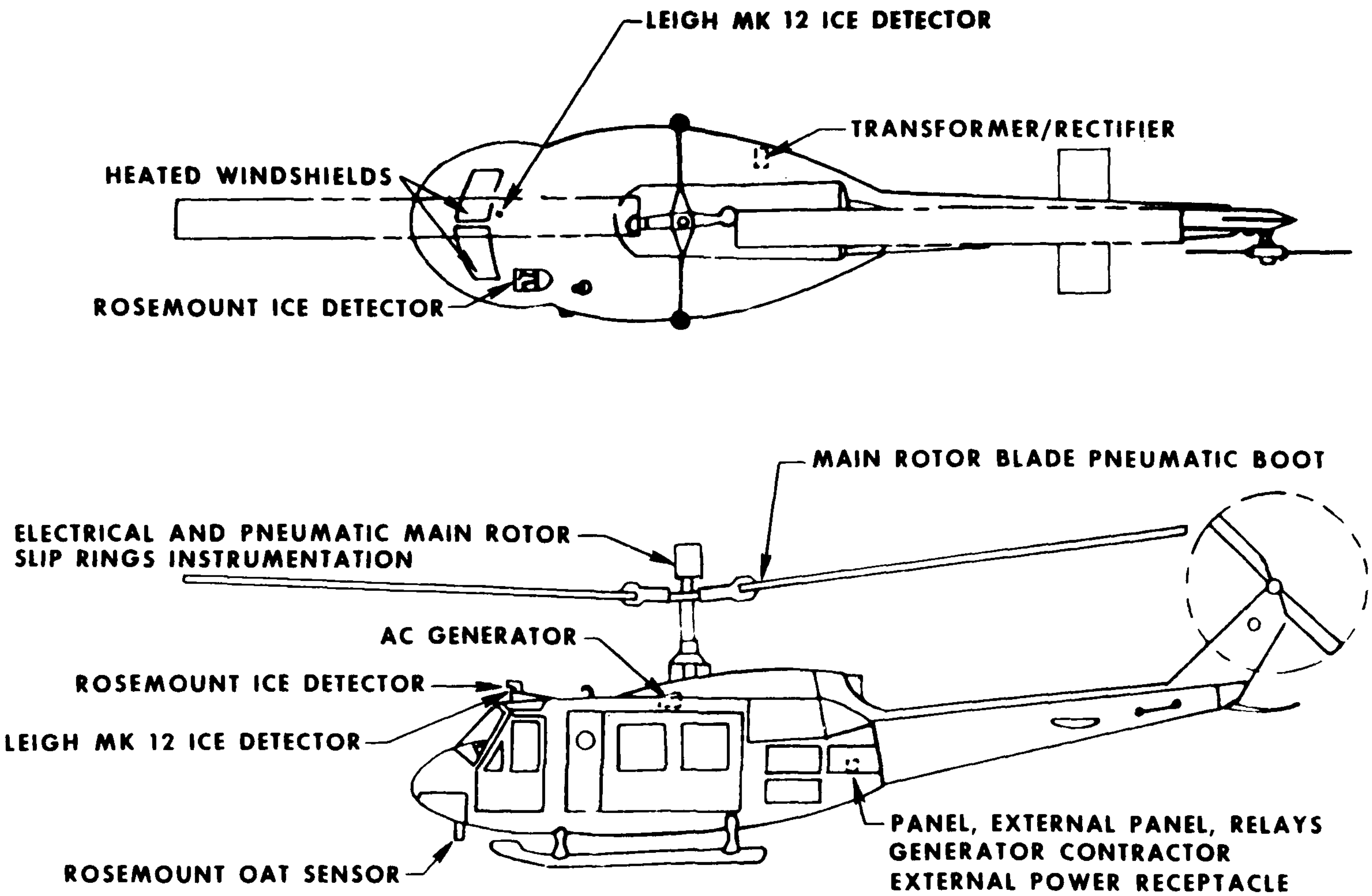

Figure B-3. Non-Standard Features

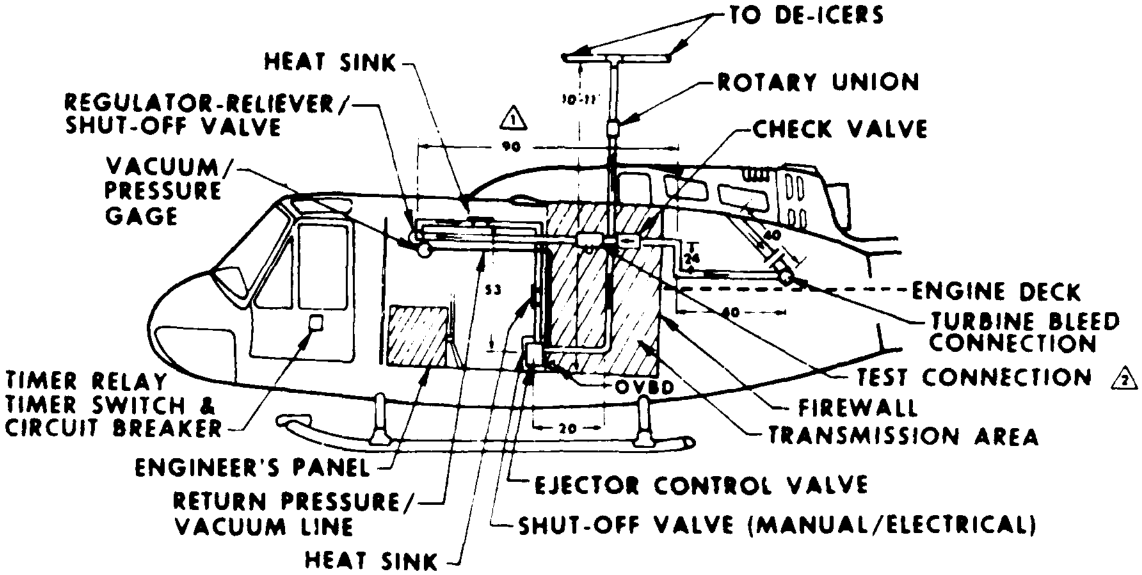

NOTES:

1. PLUMBING LENGTH DIMENSIONS ARE APPROXIMATE
2. FOR GROUND LEAKAGE TEST ONLY

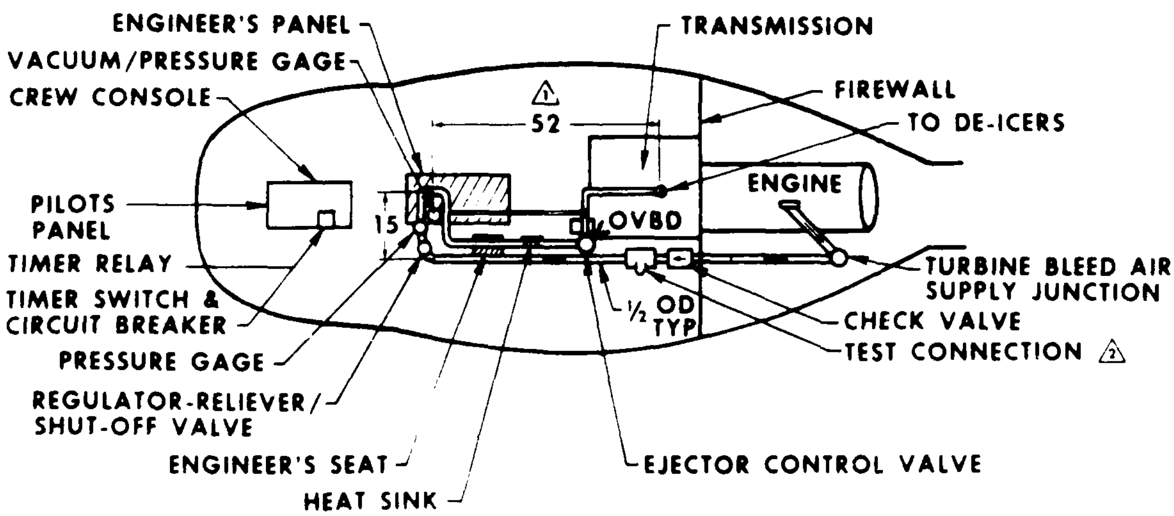

Figure B-4 Schematic of Pneumatic Deice System

shutting off inlet flow of air or preventing system pressure from rising above the system set point. The pressure-reliever is a separate spring-loaded poppet connected to a common system pressure port. The reliever is set to open and relieve pressures slightly above the system nominal pressure level. The regulated pressure was set to open at 25 psi and the reliever was set to open at 27 psi.

5. The ejector flow control valve is a three-way solenoid valve with the deicer connected to the common port. In the deenergized condition, the deicer port is connected to the exhaust port through an internal ejector. System air pressure is connected to the inlet port which has an orifice that operates the ejector to supply vacuum to the deicer. When electrical power is applied to the valve's direct-acting solenoid, the valve mechanism shifts to shut-off vacuum supply air and to direct inlet air through the deicer port to inflate the deicer. When electrical power is removed from the valve solenoid, the valve mechanism shifts to connect the deicer port to the exhaust port and vacuum is reapplied to the deicer. Modifications were made to a 3D2331 ejector flow control valve to increase the vacuum to 18 inches of mercury with a 25-psi inlet pressure.

6. The control switch is a single pole, momentary contact, toggle switch with screw terminals. The contacts are rated at 15 amps at 125 VAC or 10 amps at 250 VAC. This switch starts the timer for the single deicer inflation period.

7. The rotating union is a single pass, straight-through air union, with two single-row ball bearings. The union utilizes a balanced carbon-steel-to-carbon-graphite floating seal with "O" ring. The union is rated by the manufacturer at 1000 revolutions per minute (rpm) and 150 psi maximum.

8. The deicer hose (B-118) is a wire-reinforced neoprene and fabric construction. The hose is modified with a flap constructed of rubber with fabric covering top and bottom. The flap is used to attach the hose to the rotor blade surface. The deicer hose is attached to the drag link using nylon cable ties (TY-RAP, P/N TY-527M, Per MIL-S-23190 and MIS17332).

9. The pneumatic deicer timer is an electrical-mechanical timing device utilizing a relay to provide a single timed output of electrical power to the ejector flow control valve solenoid. When the timer is actuated through the control switch, the solenoid in the ejector flow control valve controlling air flow is immediately energized for the inflation period. At the end of the deicer inflation period, the solenoid is deenergized allowing the air to be evacuated from the deicers.

10. If the control switch is depressed for more than the preset deicer inflation period, the timer will deenergize at the end of the period. The control switch must be released and depressed again to start another inflation period.

11. Two modifications were made to the B.F. Goodrich Company (BFG) time module: (1) time period was made adjustable from 0.5 to 3.5 seconds, and (2) the module was encased for environmental protection.

12. The pneumatic deicer consists of a smooth rubber and fabric blanket containing two small spanwise deicing tubes along the leading edge, with the balance of the deicer

consisting of smaller chordwise deicing tubes. All tubes in each deicer are simultaneously inflated through a single air connection located on the "breeze side" of the deicer. The deicer is cement bonded to the airfoil leading edge. The "breeze side" of the deicer incorporates a 0.025-inch ply of BFG polyurethane (ESTANE ®) to resist weathering and abrasion. To aid application to the blade, a centerline leading edge reference line is included on the back of each deicer. The deicers are designed to operate at 25 psi (nominal) and to be installed over the basic airfoil. A molded nose piece is installed on the leading edge of the UH-1 blade under the pneumatic deicer. The purpose of the nose piece is to make the airfoil section as nearly identical to that of a standard UH-1 blade section as possible.

13. Deicing action is provided by pressurizing the stretchable deicing tubes with compressed air. The inflation of the tubes produces cracking and shearing stresses in the ice causing it to be broken into pieces and break its bond with the deicer surface. The scavenging effects of the air stream and centrifugal forces then remove the ice particles. When the ejector flow control valve is deenergized, the vacuum is applied to the deicer tubes. This is necessary to resist negative aerodynamic pressures and to maintain the tubes in a flat or deflated condition.

14. The second-generation deicing boot was modified by removing the existing deicer/erosion materials from the outboard 41 inches (station 247.0 to station 288.0) of the rotor blade. The blade leading edge surface from station 273.0 to station 288.0 (15 inches) was restored to the bare surface condition. The existing deicer/erosion materials between the end of the 15-inch bare blade section and station 247.0 were replaced with a .175-inch thick erosion material with a leading edge radius that matches that of the bare blade. A more detailed description of the boot modifications is contained in reference 5, appendix A.

15. The AC electrical system of the Kit A-equipped aircraft consists of a 30-KVA alternator, a 200-amp AC-to-DC converter, and associated control and distribution changes. The standard 28-VDC generator and quill assembly of the UH-1 has been replaced by a 30-KVA three-phase, 400-Hertz, Bendix alternator which is driven at 1200 rpm by an offset quill and gear assembly. A 200-amp AC-to-DC converter powered by the alternator has been added as a standby DC power source. The distribution and control system has been modified to make the starter generator the main DC power source.

16. The pilot and copilot windshields are anti-iced by supplying electrical power to a transparent metallic conductive coating bonded between the laminations of the windshield. Windshield heating is controlled by independent ON/OFF switches (fig. B-5). Control of windshield heat is automatic when windshield anti-ice switches are turned on. Three-phase AC power is used for heating, with a single phase heating each third of the windshield. A temperature sensor located in each windshield provides temperature input to maintain a predetermined temperature range by cyclic control of power to the heating elements.

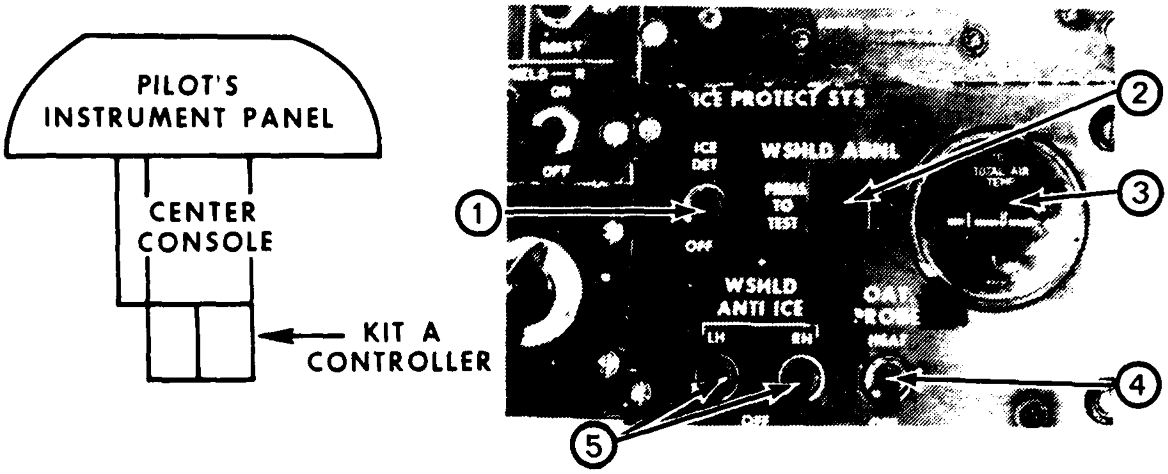

KIT A ICE PROTECTION SYSTEM PANEL		
INDEX	SWITCH OR INDICATOR	FUNCTION
1	Ice Detector On-Off	Turns on the Rosemount Ice Detector
2	WSHLD ABNL	Warning lights indicate "left" or "Right" heated glass window abnormal conditions.
3	Total Air Temperature Gage	Displays outside air temperature digitally in degrees centigrade
4	OAT Probe Heat On-Off	Provides on-off control of anti-ice heaters on the Rosemount total air temperature probe (Model 102). (Not used in conjunction with non-deiced Model 172 temperature probe).
5	WSHLD Anti-Ice On-Off	Turns on the automatic windshield deice heater controls

Figure B-5. Kit A Controller Panel

17. An ultrasonic ice detector manufactured by Rosemount Engineering, Inc. is located at the copilot's air inlet on the cabin roof. The icing signal is displayed on a liquid water content (LWC) indicator located on the center console.

18. A Leigh MK 12 ice detector is located on the cabin roof at the pilot's air inlet. A LWC display in grams per cubic meter (gm/m^3) is provided.

19. The outside air temperature sensor is an unheated resistance-type detector manufactured by Rosemount. A digital temperature display is located on the center console.

20. The FM antenna has been canted outboard (42.5 degrees from the vertical position) to prevent tail rotor contact if ice-induced oscillations occur.

APPENDIX C. INSTRUMENTATION

GENERAL

1. The airborne data acquisition system, except for the load strain gages and slipring assembly, was installed, calibrated, and maintained by AEFA personnel. The load strain gages and slipring assembly were installed by BHTI personnel. Data was obtained from calibrated instrumentation and displayed in the cockpit, recorded on magnetic tape and, during the loads survey only, telemetered to a ground station for real-time safety-of-flight monitoring. The cockpit instrument panels are shown in figures C-1 and C-2. A test instrumentation boom was mounted at the base of the aircraft windshield and extended 94 inches forward of the nose of the aircraft. A swiveling pitot-static tube and angle of attack and sideslip vanes were mounted on the boom, as shown in figure C-3. Instrumentation and related special equipment installed in the aircraft and used for this test are:

Pilot's and Copilot's Panel

Airspeed (boom)
Pressure altitude (boom)
Airspeed (ship's)
Pressure altitude (ship's)
Fuel quantity used
Angle of sideslip
Engine torque (calibrated sensitive)
Engine torque (ship's)

Engineer's Panel

Reference time of day
Main rotor speed
Free air total temperature
Ejector control valve regulated pressure
Deicer boot vacuum/pressure

Magnetic Tape

2. The following parameters were recorded on magnetic tape throughout the project.

Record number
Time of day
Airspeed (boom)
Pressure altitude (boom)
Angle of attack
Angle of sideslip
Control positions
- Longitudinal
- Lateral
- Directional
- Collective

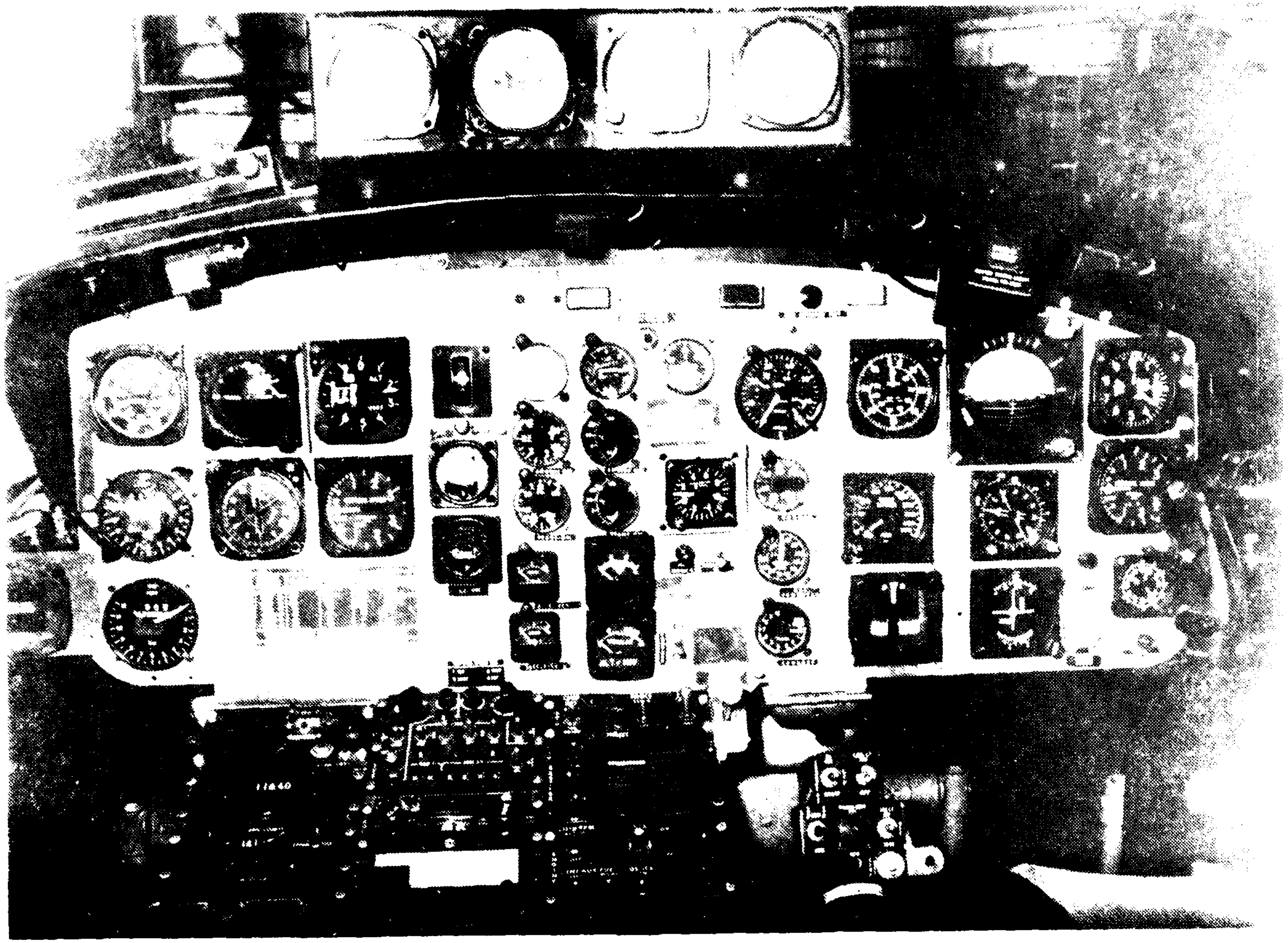

Figure C-1. Pilot and Copilot's Instrument Panel

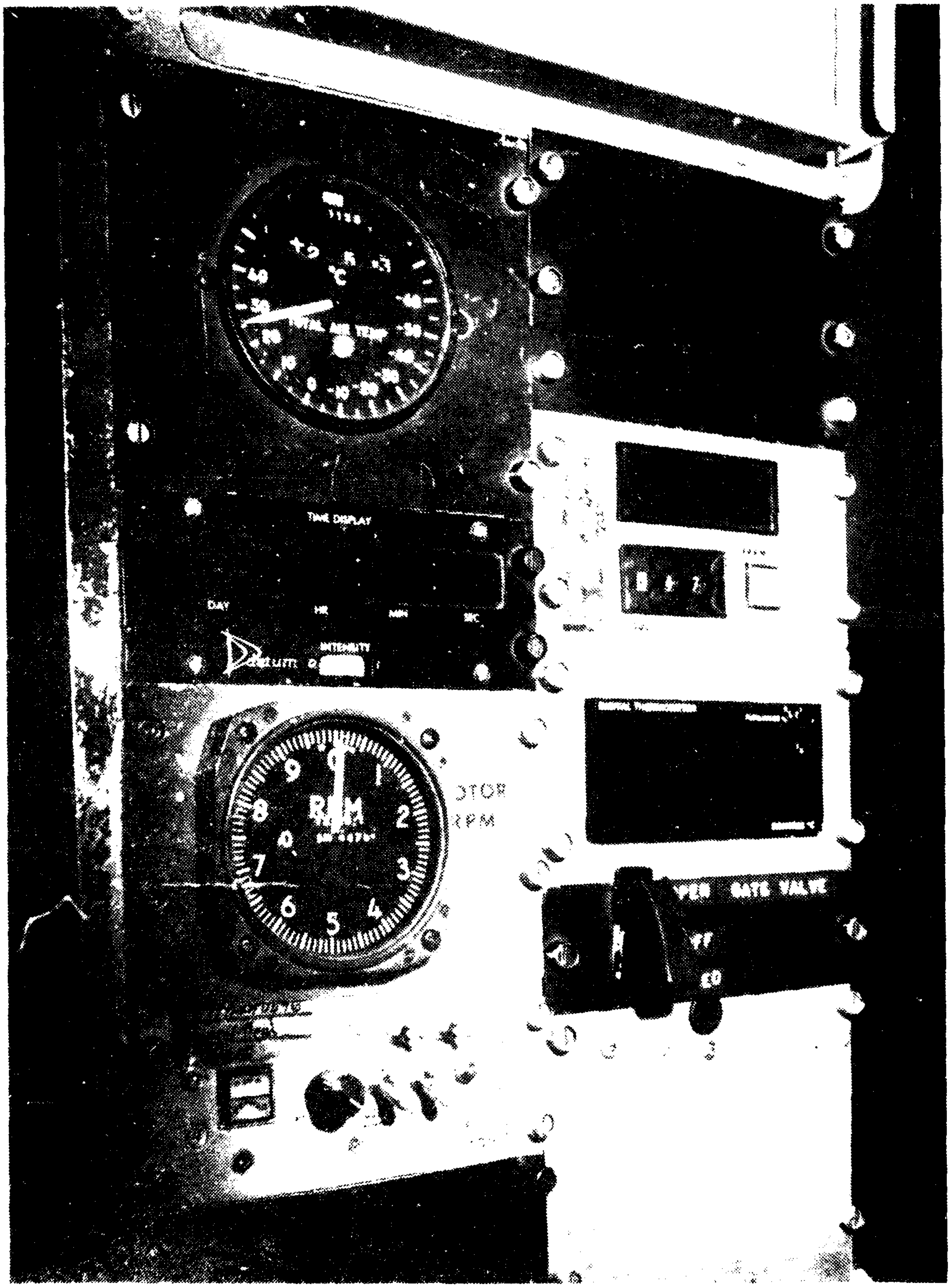
°C
TOTAL AIR TEMP
TIME DISPLAY
DAY
HR
MIN
SEC
Datum
INTENSITY
RPM
GATE VALVE

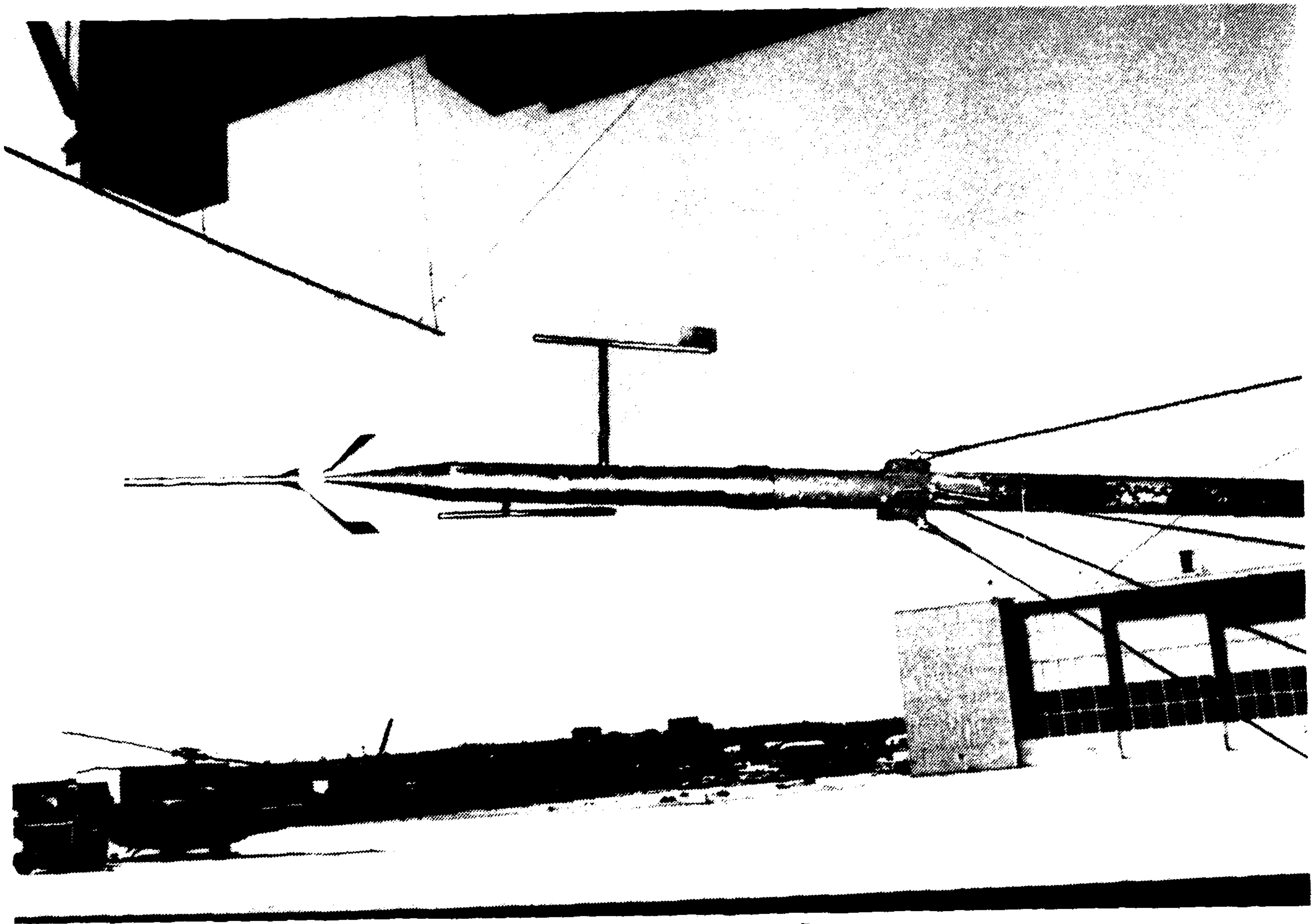

Figure C-3. Test Instrumentation Boom

Aircraft Attitudes
Roll
Pitch
Aircraft Heading
Aircraft rates
Roll
Pitch
Yaw
Center of gravity normal acceleration
Fuel flow
Fuel quantity used
Free air total temperature
Main rotor speed
Engine torque

3. The following parameters were recorded on magnetic tape during the loads survey only.

Main rotor mast torque
Main rotor mast bending parallel
Main rotor mast bending perpendicular
Main rotor blade beam and chord bending at the following stations:
Station 35
Station 84
Station 150
Main rotor blade beam bending at stations 192 and 234
Bleed air pressure upstream of ejector flow control valve
Bleed air pressure downstream of ejector flow control valve

Magnetic Tape and Telemetered Data

4. The following parameters were recorded on magnetic tape and telemetered to a ground station for real-time safety-of-flight monitoring during the loads survey only.

No. 1 flight control actuator axial load
No. 2 flight control actuator axial load
No. 3 flight control actuator axial load
Main rotor pitch link axial force
Hub beam bending at station 5.5
Hub chord bending at station 5.5
Main rotor blade chord bending at station 192

Pitot-Static Calibration

5. The results of the test boom airspeed system calibration performed for AEFA Project No. 83-13 were used for this evaluation. The calibration of the test boom airspeed system is presented in figure C-4. The altimeter position error was calculated assuming all airspeed position error occurred at the static source.

FIGURE C-4

AIRSPEED CALIBRATION
JUH-1H USA S/N 70-16318
BOOM SYSTEM POSITION ERROR

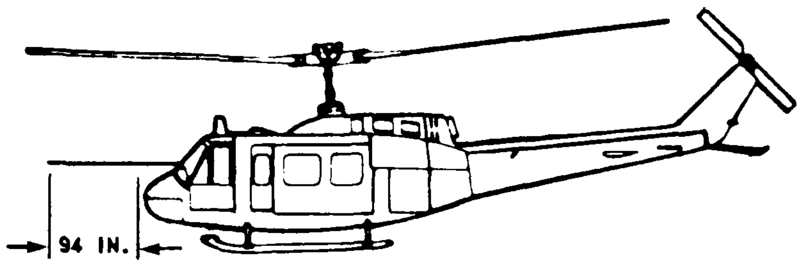

NOTE: TRAILING BOMB METHOD

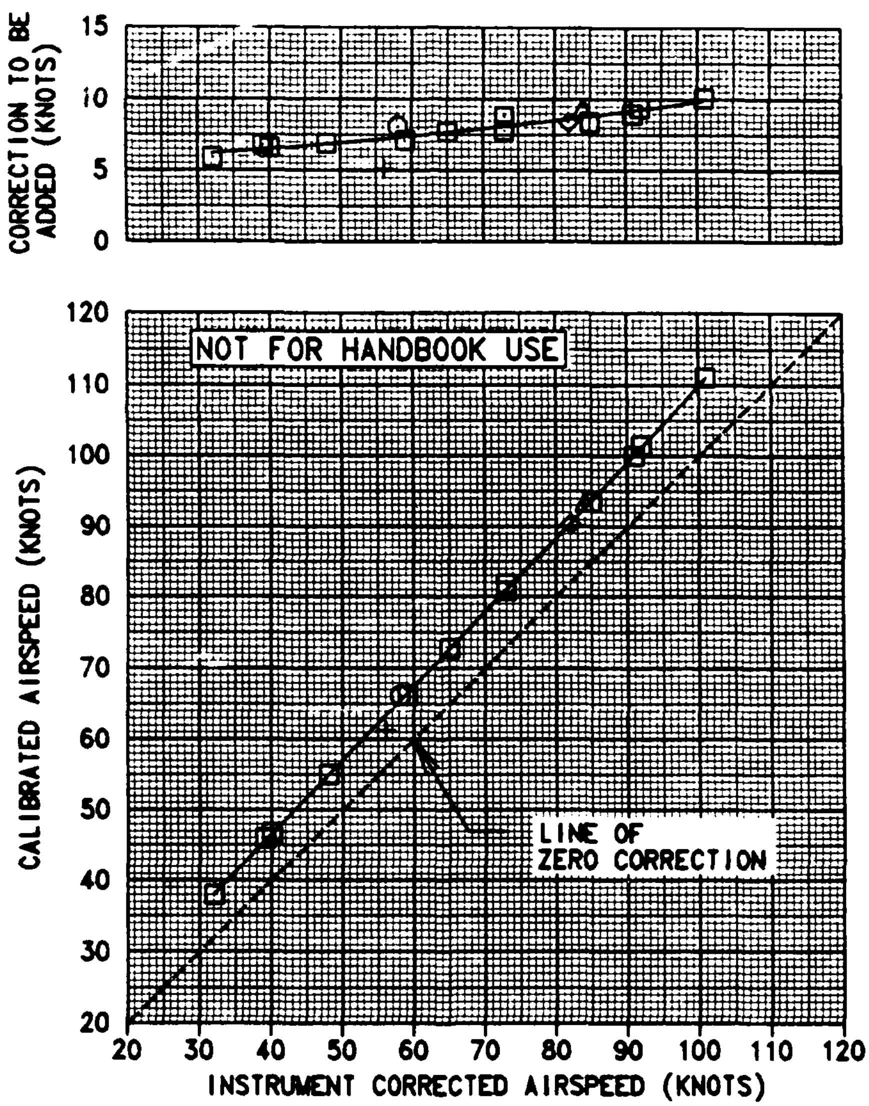

Engine Calibration

6. The hover and low-speed flight portions of the structural loads survey and a small part of the level flight portion of the structural loads survey were performed with T53-L-13B S/N LE20825B installed in the helicopter. This engine was then replaced with T53-L-13B S/N LE20221B. The remainder of the loads survey, and the level flight performance evaluation, were performed with T53-L-13B S/N LE20221B installed in the helicopter. T53-L-13B S/N LE20221B was calibrated in a test cell at the Corpus Christi Army Depot before commencement of the level flight performance evaluation. The following data were obtained at each point during the calibration.

Engine gas producer speed
Engine output shaft speed
Engine output shaft torque
Engine torquemeter pressure
Gearbox pressure
Engine exhaust gas temperature
Fuel flow
Test cell ambient temperature
Test cell ambient pressure

The relationship between differential torque pressure (torquemeter pressure minus gearbox pressure) and engine torque determined from this calibration was used to determine engine torque during the evaluation. The relationship is presented in figure C-5.

FIGURE C-5

ENGINE TORQUEMETER CALIBRATION

T53-L-13B S/N LE20221B

SYMBOL	OUTPUT SHAFT SPEED (RPM)	DATA SOURCE
○	6600	ENGINE TORQUEMETER CALIBRATION
□	6400	FROM TEST CONDUCTED AT CORPUS
◇	6000	CHRISTI ARMY DEPOT 17 DEC 87.

NOTE: DIFFERENTIAL PRESSURE, ΔP = TORQUEMETER PRESSURE MINUS GEARBOX PRESSURE.

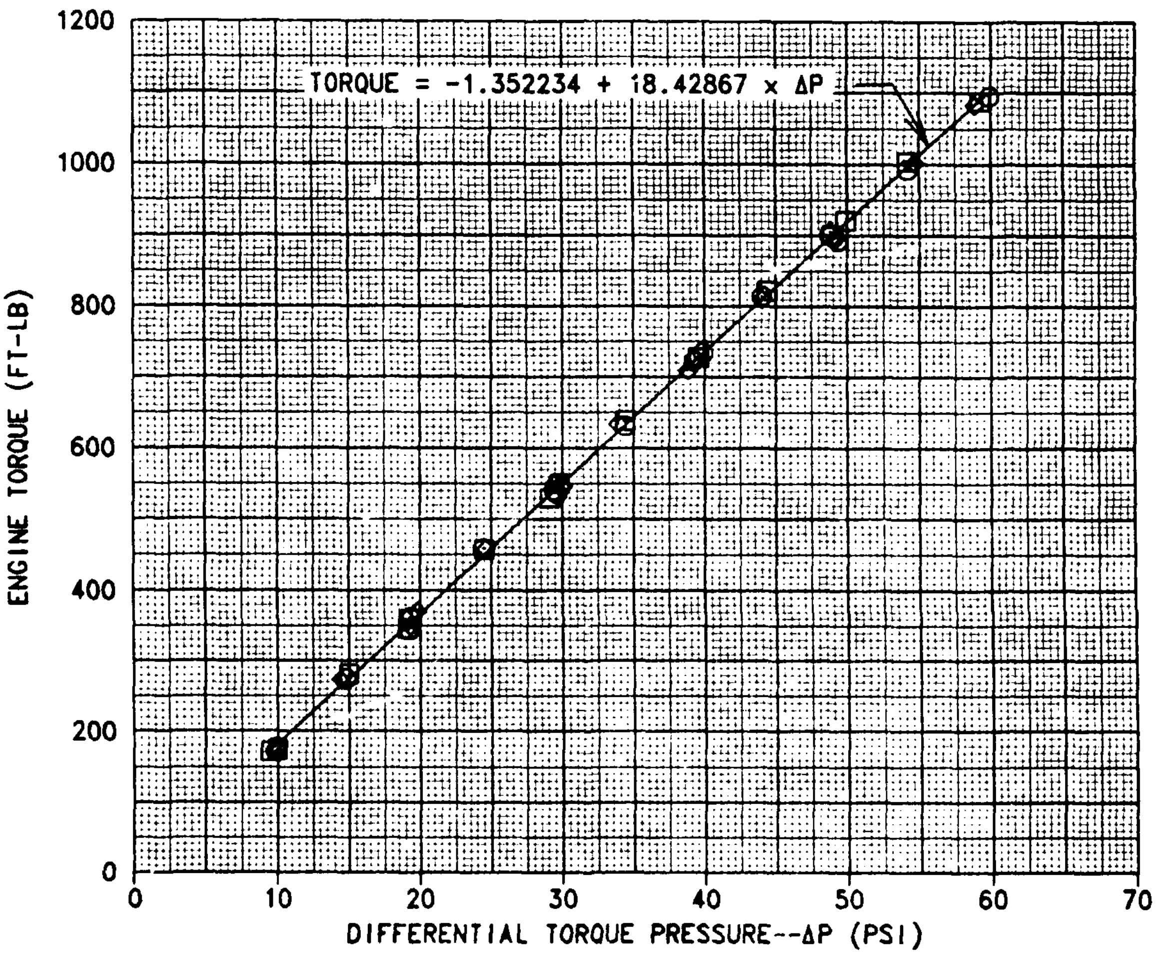

APPENDIX D. TEST TECHNIQUES AND DATA ANALYSIS METHODS

1. Reference 2, appendix A was used as a guide for evaluation purposes. Critical loads parameters indicated in appendix C were telemetered to a ground station for real-time safety of flight monitoring by an AEFA engineer for structural loads testing. The critical loads parameters were monitored and analyzed during hover, low-speed, level flight, climbs and descents, autorotational entries, turns, and inflight dynamic system-engine compatibility tests.

2. The aircraft empty weight (including full oil and fuel) and longitudinal center of gravity (cg) location were previously determined with a portable electronic weighing kit.

3. A manometer-type external sight gauge was calibrated and used to determine fuel volume. Fuel specific gravity was measured with a hydrometer. The fuel loading for each test flight was determined both before engine start and following engine shutdown. Fuel used in flight was recorded manually from a test fuel used system and compared with the preflight and postflight sight gauge readings. Fuel cg as a function of fuel volume contained in the fuel cell (209-gallon capacity) had been previously determined. This relationship was used to calculate aircraft cg for each test point. Aircraft gross weight and cg were also controlled by ballast installed in the aircraft.

4. The level flight performance data were generalized by the following nondimensional coefficients:

a. Coefficient of power (C_P):

$$C_P = SHP \frac{(550)}{\rho A (\Omega R)^3} \tag{1}$$

b. Coefficient of thrust (C_T):

$$C_T = \frac{GW}{\rho A (\Omega R)^2} \tag{2}$$

c. Advance ratio (μ):

$$\mu = \frac{V_T \ (1.68781)}{\Omega R} \tag{3}$$

d. Advancing blade tip mach number (M_{tip}):

$$M_{tip} = \frac{V_T(1.68781) + (\Omega R)}{a} \tag{4}$$

e. Referred rotor speed = $N_R/\sqrt{\theta}$

Where:

SHP = Engine output shaft horsepower (shp)

ϱ = Ambient air density (lb-sec²/ft⁴)

A = Main rotor disc area (ft²) = 1809.56

Ω = Main rotor angular velocity (radians/sec)

R = Main rotor radius (ft) = 24.000

GW = Gross weight (lb)

$$V_T = \text{True airspeed (kt)} = \frac{V_E}{1.68781\sqrt{\varrho/\varrho_o}}$$

1.68781 = Conversion factor (ft/sec-kt)

ϱ_o = 0.0023769 (lb-sec²/ft⁴)

V_E = Equivalent airspeed (ft/sec) =

$$\left\{7(70.7262)\frac{P_a}{\varrho_o}\left[\left(\frac{Q_c}{P_a}+1\right)^{2/7}-1\right]\right\}^{1/2}$$

70.7262 = Conversion factor (lb/ft²-in.-Hg)

Q_c = Dynamic pressure (in.-Hg)

P_a = Ambient air pressure (in.-Hg)

a = Speed of sound (ft/sec) = $1116.45\sqrt{\theta}$

θ = $(T_a + 273.15)/288.15$

T_a = Ambient air temperature (deg C)

N_R = Main rotor speed (rpm)

5. The engine output shaft torque was determined from the engine manufacturer's torque system. The relationship of measured torque pressure to engine output shaft torque was determined from the engine test cell calibration presented in figure C-5, appendix C as follows:

$$Q = -1.352234 + 18.42867 \times \Delta P$$

Where:

Q = Engine output shaft torque (ft-lb)

ΔP = Torquemeter pressure minus gearbox pressure (lb/ft²)

6. Engine output shaft power was determined by the following equation:

$$SHP = (2\pi)N_P \frac{Q}{33,000} = \frac{N_P(Q)}{5252.113}$$

Where:

N_P = Engine output shaft rotational speed (rpm)
33,000 = Conversion factor (ft-lb/min-SHP)

7. Each level flight performance test point was flown in zero-sideslip flight at a predetermined C_T and referred rotor speed ($N_R/\sqrt{\theta}$). To maintain a constant ratio of gross weight to pressure ratio (W/δ), altitude was increased as fuel was consumed. To maintain a constant referred rotor speed, actual rotor speed was varied as ambient temperature varied.

8. Test-day level flight data was corrected to average test-day conditions as follows:

$$V_{T_s} = V_{T_t}\left(\frac{N_{R_s}}{N_{R_t}}\right)$$

$$SHP_s = SHP_t\left(\frac{\rho_s}{\rho_t}\right)\left(\frac{N_{R_s}}{N_{R_t}}\right)^3$$

Where:

Subscript s = Average test day
Subscript t = Test day

9. Specific range was derived from level flight power required and fuel flow. Referred shaft power and referred fuel flow were calculated as follows:

$$\text{Referred Shaft Power} = \frac{SHP_t}{(\delta)(\theta)^{0.587}}$$

$$\text{Referred Fuel Flow} = \frac{W_{f_t}}{(\delta)(\theta)^{0.712}}$$

Where:

$\delta = P_a/29.92125$
W_f = Fuel flow rate (lb/hr)

A curve fit was applied to this referred data and used to correct test day fuel flow to average test day fuel flow as follows:

$$W_{f_s} = W_{f_t} + \Delta W_f$$

Where:

ΔW_f = Change in fuel flow between SHP_t and SHP_s

Specific Range was calculated as follows:

$$SR = \frac{V_{T_s}}{W_{f_s}}$$

Where:

SR = Specific range (nautical air miles/lb fuel)

Test data corrected to average test day conditions is presented in figures E-3 through E-5 and E-13.

10. Level flight data was analyzed by use of a simulated three-dimensional plot (C_T and μ versus C_P) for each configuration. The reduction of these plots to a family of curves of C_T versus C_P for constant values of μ allows determination of power required as a function of airspeed for any value of C_T.

11. The Handling Qualities Rating Scale presented in figure D-1 was used to augment pilot comments relative to handling qualities and workload.

DEFINITION

12. A shortcoming is defined as an imperfection or malfunction occurring during the life cycle of equipment which must be reported and which should be corrected to increase efficiency and to render the equipment completely serviceable. It will not cause an immediate breakdown, jeopardize safe operation, or materially reduce the usability of the material or end product.

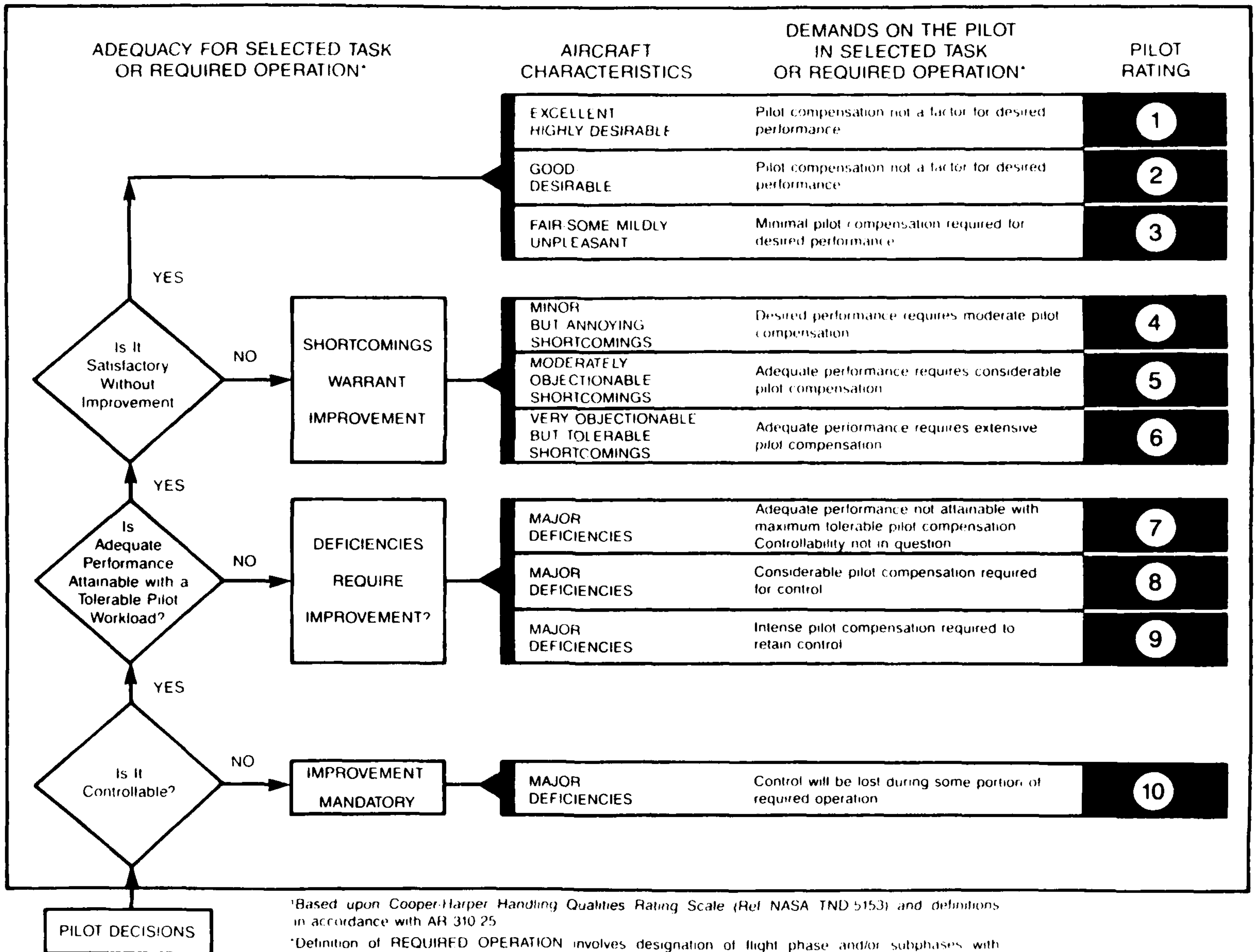

*Based upon Cooper-Harper Handling Qualities Rating Scale (Ref NASA TND 5153) and definitions in accordance with AR 310 25

*Definition of REQUIRED OPERATION involves designation of flight phase and/or subphases with accompanying conditions

Figure D-1. Handling Qualities Rating Scale

APPENDIX E. TEST DATA

INDEX

FIGURE E-1

NONDIMENSIONAL LEVEL FLIGHT PERFORMANCE
JUH-1H USA S/N 70-16318
MODIFIED SECOND-GENERATION PNEUMATIC BOOT DEICING SYSTEM

NOTES:
1. PBDS DEFLATED
2. ZERO SIDESLIP
3. AVERAGE REFERRED ROTOR SPEED = 319.8 RPM
4. AVERAGE LONGITUDINAL CG AT FS 134.3
5. AVERAGE LATERAL CG AT BL 0.2 LEFT
6. POINTS DERIVED FROM FIGURES E-3 THROUGH E-5
7. DASHED LINE INDICATES EXTRAPOLATED DATA

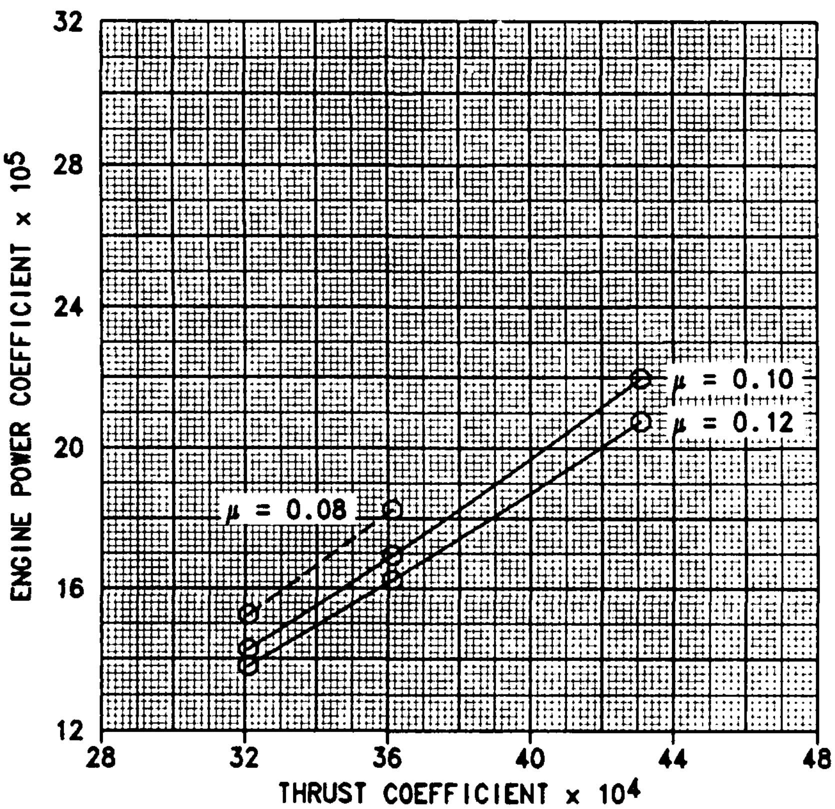

FIGURE E-2

NONDIMENSIONAL LEVEL FLIGHT PERFORMANCE

JUH-1H USA S/N 70-16318

MODIFIED SECOND-GENERATION PNEUMATIC BOOT DEICING SYSTEM

NOTES:
1. PBDS DEFLATED
2. ZERO SIDESLIP
3. AVERAGE REFERRED ROTOR SPEED = 319.8 RPM
4. AVERAGE LONGITUDINAL CG AT FS 134.3
5. AVERAGE LATERAL CG AT BL 0.2 LEFT
6. POINTS DERIVED FROM FIGURES E-3 THROUGH E-5

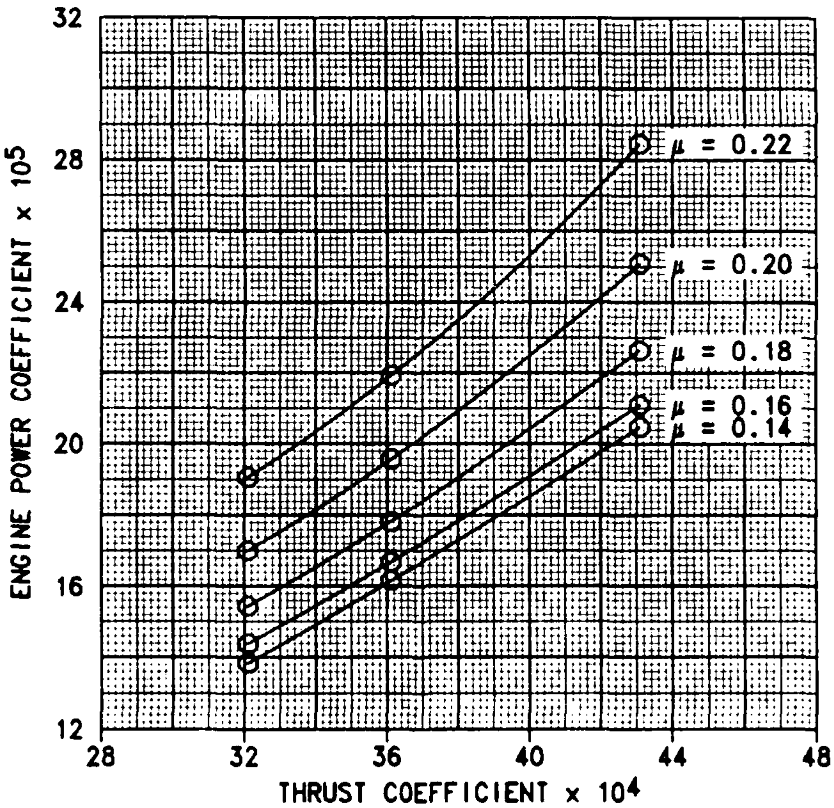

FIGURE E-3

LEVEL FLIGHT PERFORMANCE
JUH-1H USA S/N 70-16318
MODIFIED SECOND-GENERATION PNEUMATIC BOOT DEICING SYSTEM

AVG GROSS WEIGHT (LB)	AVG CG LOCATION LONG (FS)	AVG CG LOCATION LAT (BL)	AVG DENSITY ALTITUDE (FT)	AVG OAT (DEG C)	AVG REFERRED ROTOR SPEED (RPM)	AVG C_T $\times 10^4$	CONFIGURATION
7520	136.1	0.8 RT	5550	13.5	319.8	32.10	PBDS DEFLATED

NOTES: 1. AVERAGE ROTOR SPEED = 319 RPM
2. ZERO SIDESLIP

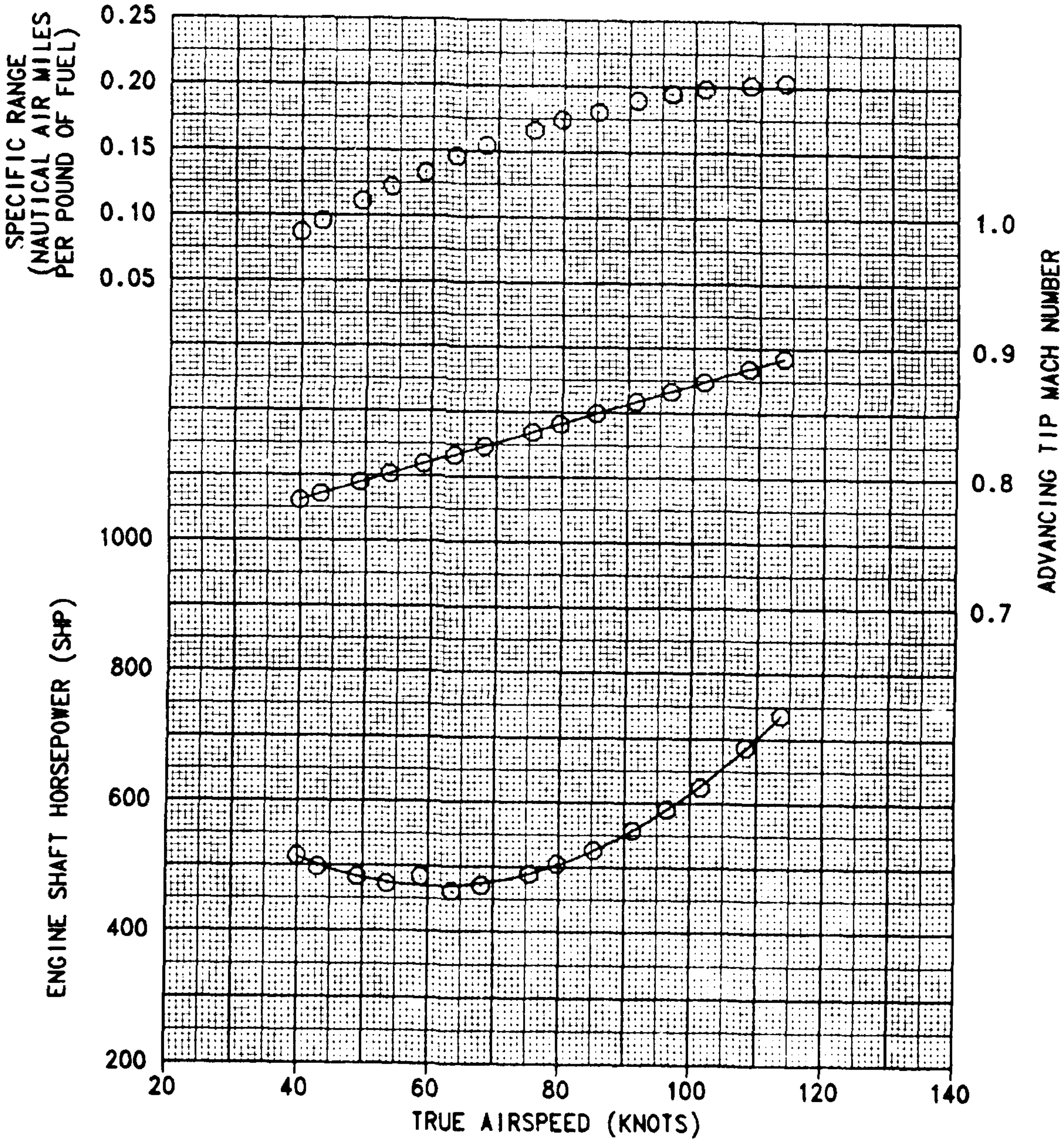

FIGURE E-4

LEVEL FLIGHT PERFORMANCE
JUH-1H USA S/N 70-16318
MODIFIED SECOND-GENERATION PNEUMATIC BOOT DEICING SYSTEM

AVG GROSS WEIGHT (LB)	AVG CG LOCATION LONG (FS)	AVG CG LOCATION LAT (BL)	AVG DENSITY ALTITUDE (FT)	AVG OAT (DEG C)	AVG REFERRED ROTOR SPEED (RPM)	AVG C_T $\times 10^4$	CONFIGURATION
8020	133.3	1.3 LT	7100	12.0	319.8	36.12	PBDS DEFLATED

NOTES: 1. AVERAGE ROTOR SPEED = 318 RPM
2. ZERO SIDESLIP

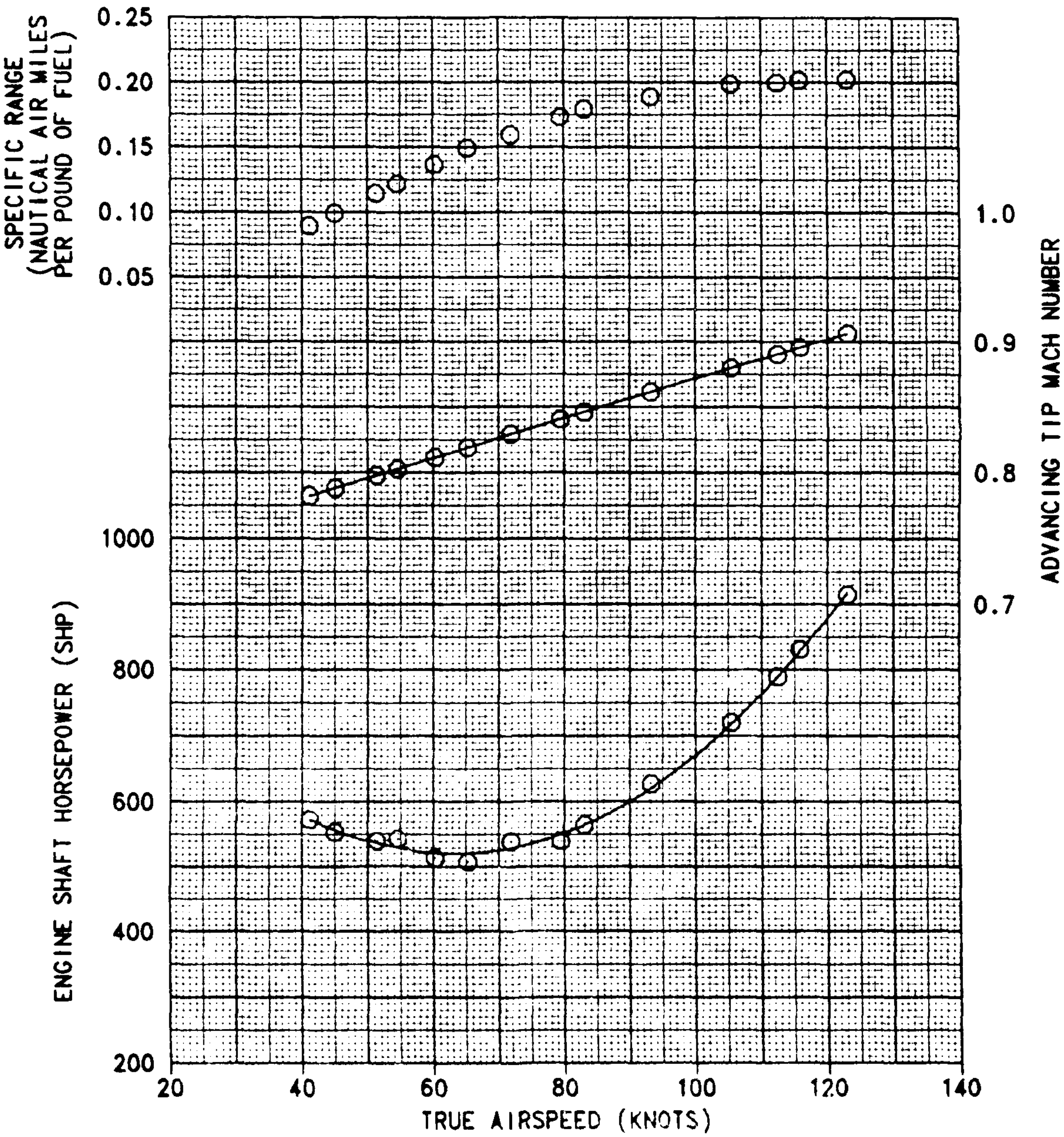

FIGURE E-5

LEVEL FLIGHT PERFORMANCE
JUH-1H USA S/N 70-16318
MODIFIED SECOND-GENERATION PNEUMATIC BOOT DEICING SYSTEM

AVG GROSS WEIGHT (LB)	AVG CG LOCATION LONG (FS)	AVG CG LOCATION LAT (BL)	AVG DENSITY ALTITUDE (FT)	AVG OAT (DEG C)	AVG REFERRED ROTOR SPEED (RPM)	AVG C_T $\times 10^4$	CONFIGURATION
8200	133.6	0.1 LT	11420	6.5	319.9	43.08	PBDS DEFLATED

NOTES: 1. AVERAGE ROTOR SPEED = 315 RPM
2. ZERO SIDESLIP

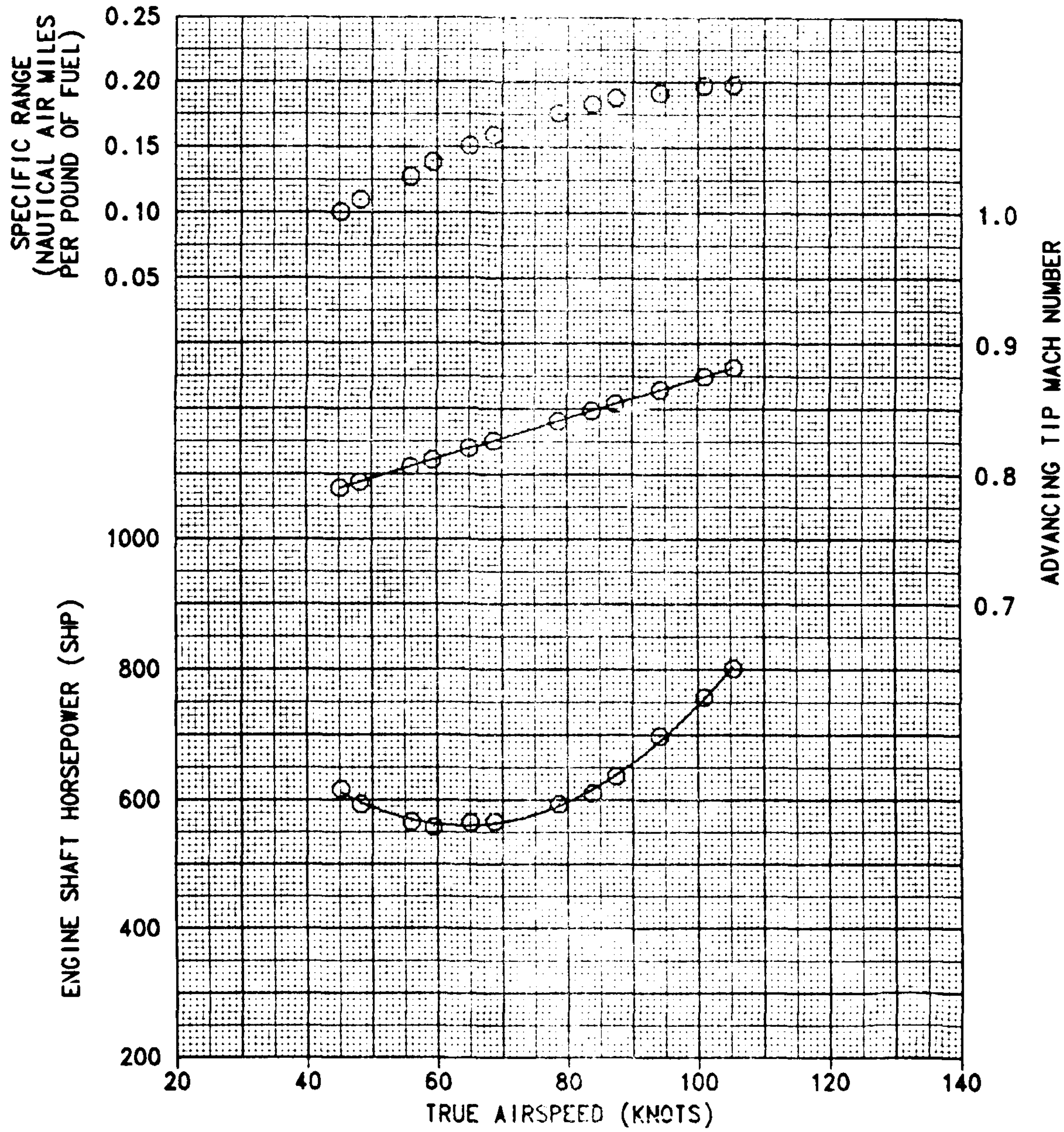

FIGURE E-6

NONDIMENSIONAL LEVEL FLIGHT PERFORMANCE

JUH-1H USA S/N 70-16318

MODIFIED SECOND-GENERATION PNEUMATIC BOOT DEICING SYSTEM
ADVANCE RATIO = 0.10

NOTES:
1. PBDS DEFLATED
2. ZERO SIDESLIP
3. AVERAGE REFERRED ROTOR SPEED = 319.8 RPM
4. AVERAGE LONGITUDINAL CG AT FS 134.3
5. AVERAGE LATERAL CG AT BL 0.2 LEFT
6. POINTS DERIVED FROM FIGURES E-3 THROUGH E-5
7. SHORT DASHES SHOW PERFORMANCE WITH UNMODIFIED SECOND-GENERATION PBDS; CURVE OBTAINED FROM USAAEFA REPORT 83-13
8. LONG DASHES SHOW PERFORMANCE WITH STANDARD BLADES; CURVE OBTAINED FROM USAAEFA REPORT 83-13

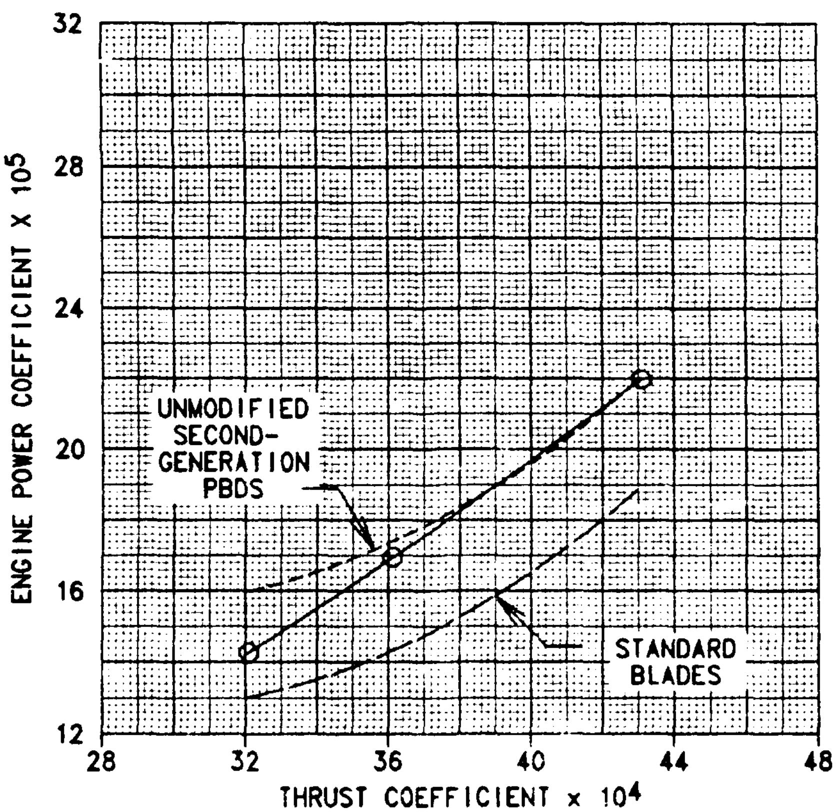

FIGURE E-7

NONDIMENSIONAL LEVEL FLIGHT PERFORMANCE

JUH-1H USA S/N 70-16318

MODIFIED SECOND-GENERATION PNEUMATIC BOOT DEICING SYSTEM
ADVANCE RATIO = 0.12

NOTES:
1. PBDS DEFLATED
2. ZERO SIDESLIP
3. AVERAGE REFERRED ROTOR SPEED = 319.8 RPM
4. AVERAGE LONGITUDINAL CG AT FS 134.3
5. AVERAGE LATERAL CG AT BL 0.2 LEFT
6. POINTS DERIVED FROM FIGURES E-3 THROUGH E-5
7. SHORT DASHES SHOW PERFORMANCE WITH UNMODIFIED SECOND-GENERATION PBDS; CURVE OBTAINED FROM USAAEFA REPORT 83-13
8. LONG DASHES SHOW PERFORMANCE WITH STANDARD BLADES; CURVE OBTAINED FROM USAAEFA REPORT 83-13

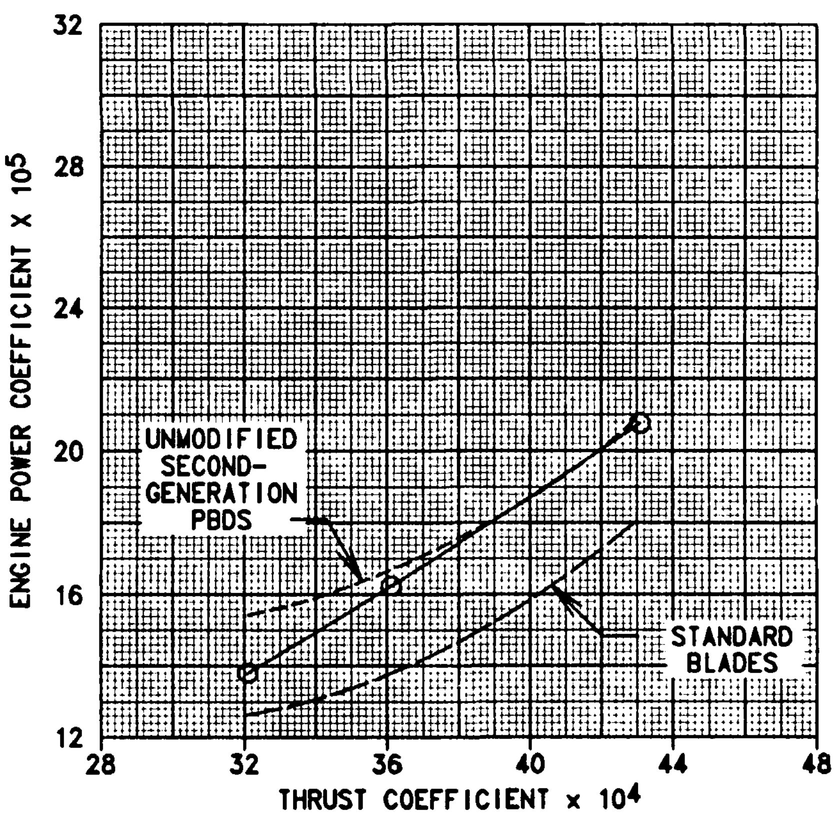

FIGURE E-8

NONDIMENSIONAL LEVEL FLIGHT PERFORMANCE

JUH-1H USA S/N 70-16318

MODIFIED SECOND-GENERATION PNEUMATIC BOOT DEICING SYSTEM

ADVANCE RATIO = 0.14

NOTES:
1. PBDS DEFLATED
2. ZERO SIDESLIP
3. AVERAGE REFERRED ROTOR SPEED = 319.8 RPM
4. AVERAGE LONGITUDINAL CG AT FS 134.3
5. AVERAGE LATERAL CG AT BL 0.2 LEFT
6. POINTS DERIVED FROM FIGURES E-3 THROUGH E-5
7. SHORT DASHES SHOW PERFORMANCE WITH UNMODIFIED SECOND-GENERATION PBDS; CURVE OBTAINED FROM USAAEFA REPORT 83-13
8. LONG DASHES SHOW PERFORMANCE WITH STANDARD BLADES; CURVE OBTAINED FROM USAAEFA REPORT 83-13

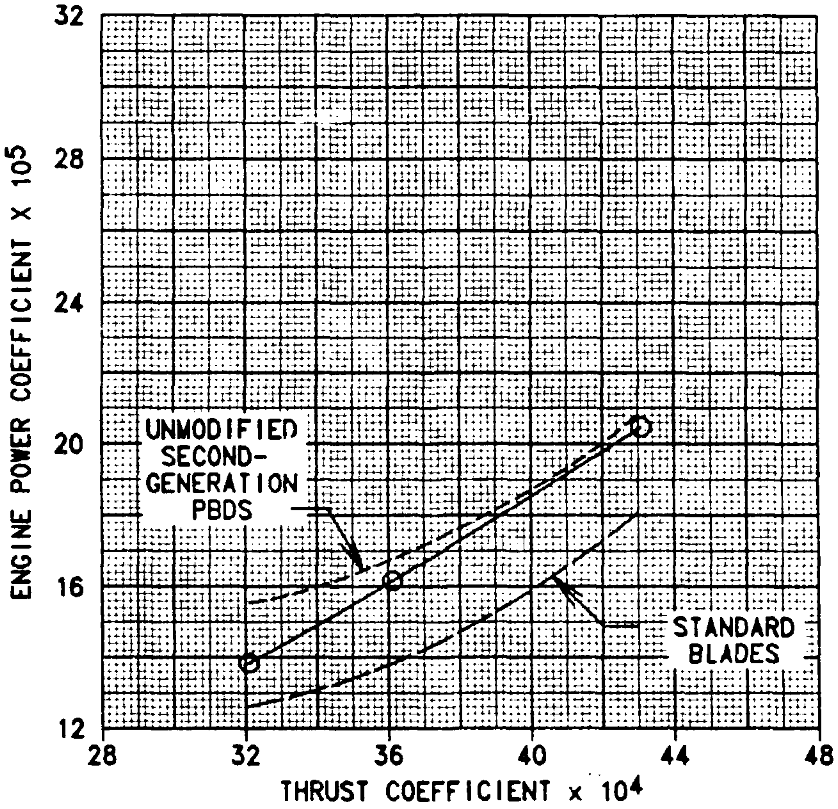

FIGURE E-9

NONDIMENSIONAL LEVEL FLIGHT PERFORMANCE

JUH-1H USA S/N 70-16318

MODIFIED SECOND-GENERATION PNEUMATIC BOOT DEICING SYSTEM
ADVANCE RATIO = 0.16

NOTES:
1. PBDS DEFLATED
2. ZERO SIDESLIP
3. AVERAGE REFERRED ROTOR SPEED = 319.8 RPM
4. AVERAGE LONGITUDINAL CG AT FS 134.3
5. AVERAGE LATERAL CG AT BL 0.2 LEFT
6. POINTS DERIVED FROM FIGURES E-3 THROUGH E-5
7. SHORT DASHES SHOW PERFORMANCE WITH UNMODIFIED SECOND-GENERATION PBDS; CURVE OBTAINED FROM USAAEFA REPORT 83-13
8. LONG DASHES SHOW PERFORMANCE WITH STANDARD BLADES; CURVE OBTAINED FROM USAAEFA REPORT 83-13

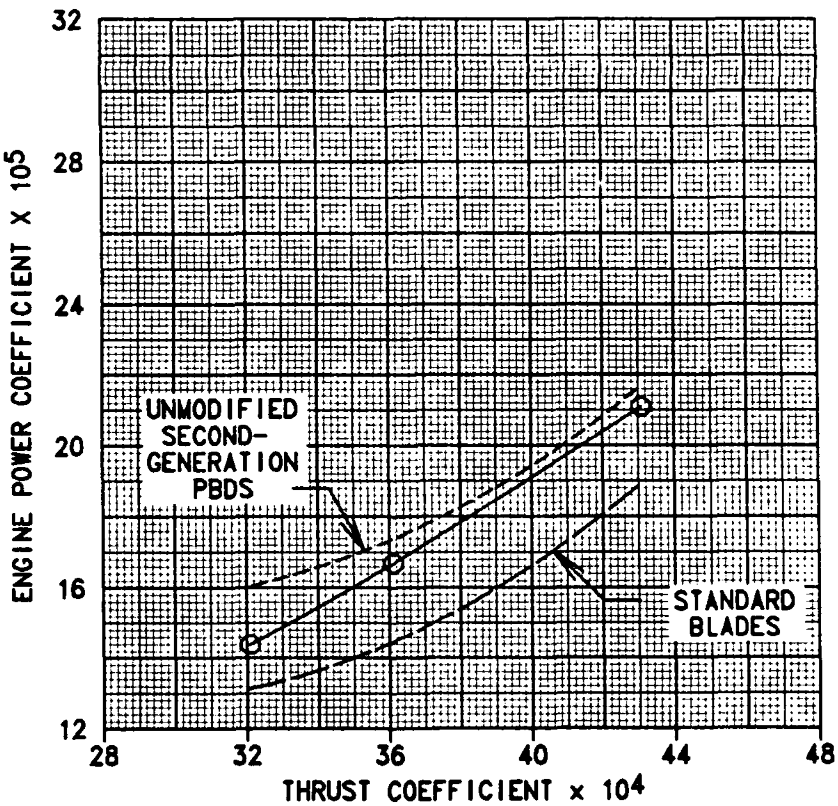

FIGURE E-10

NONDIMENSIONAL LEVEL FLIGHT PERFORMANCE

JUH-1H USA S/N 70-16318

MODIFIED SECOND-GENERATION PNEUMATIC BOOT DEICING SYSTEM
ADVANCE RATIO = 0.18

NOTES:
1. PBDS DEFLATED
2. ZERO SIDESLIP
3. AVERAGE REFERRED ROTOR SPEED = 319.8 RPM
4. AVERAGE LONGITUDINAL CG AT FS 134.3
5. AVERAGE LATERAL CG AT BL 0.2 LEFT
6. POINTS DERIVED FROM FIGURES E-3 THROUGH E-5
7. SHORT DASHES SHOW PERFORMANCE WITH UNMODIFIED SECOND-GENERATION PBDS; CURVE OBTAINED FROM USAAEFA REPORT 83-13
8. LONG DASHES SHOW PERFORMANCE WITH STANDARD BLADES; CURVE OBTAINED FROM USAAEFA REPORT 83-13

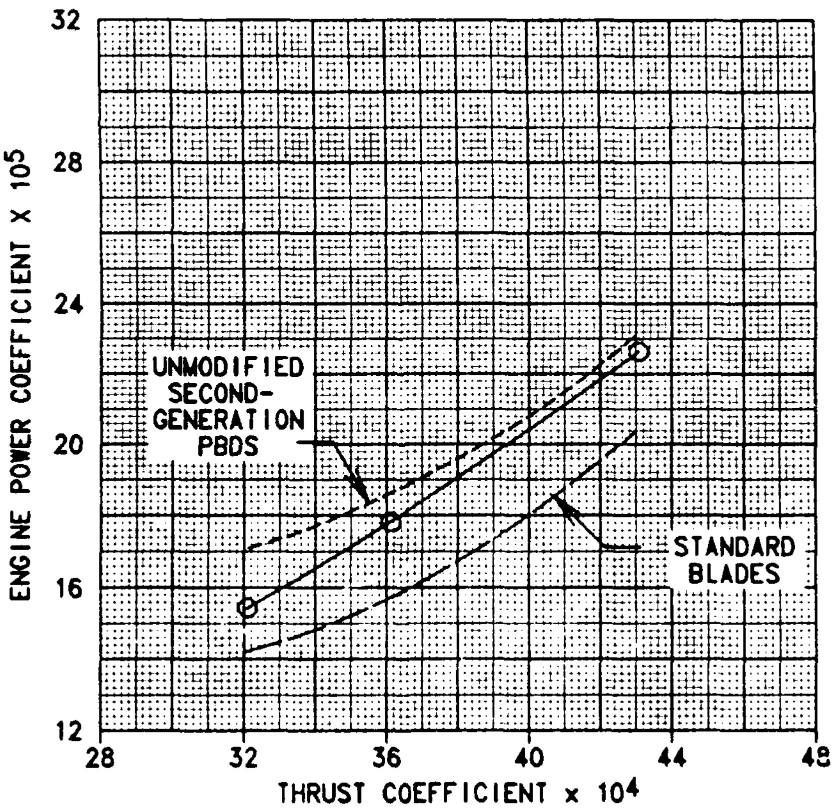

FIGURE E-11

NONDIMENSIONAL LEVEL FLIGHT PERFORMANCE

JUH-1H USA S/N 70-16318

MODIFIED SECOND-GENERATION PNEUMATIC BOOT DEICING SYSTEM
ADVANCE RATIO = 0.20

NOTES:
1. PBDS DEFLATED
2. ZERO SIDESLIP
3. AVERAGE REFERRED ROTOR SPEED = 319.8 RPM
4. AVERAGE LONGITUDINAL CG AT FS 134.3
5. AVERAGE LATERAL CG AT BL 0.2 LEFT
6. POINTS DERIVED FROM FIGURES E-3 THROUGH E-5
7. SHORT DASHES SHOW PERFORMANCE WITH UNMODIFIED SECOND-GENERATION PBDS; CURVE OBTAINED FROM USAAEFA REPORT 83-13
8. LONG DASHES SHOW PERFORMANCE WITH STANDARD BLADES; CURVE OBTAINED FROM USAAEFA REPORT 83-13

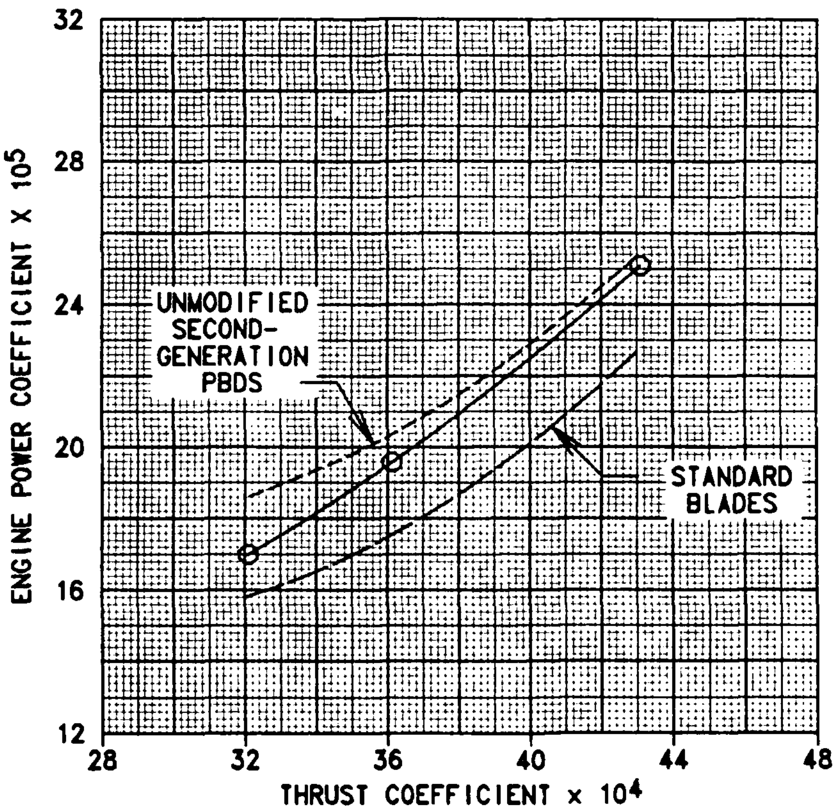

FIGURE E-12

NONDIMENSIONAL LEVEL FLIGHT PERFORMANCE

JUH-1H USA S/N 70-16318

MODIFIED SECOND-GENERATION PNEUMATIC BOOT DEICING SYSTEM
ADVANCE RATIO = 0.22

NOTES:
1. PBDS DEFLATED
2. ZERO SIDESLIP
3. AVERAGE REFERRED ROTOR SPEED = 319.8 RPM
4. AVERAGE LONGITUDINAL CG AT FS 134.3
5. AVERAGE LATERAL CG AT BL 0.2 LEFT
6. POINTS DERIVED FROM FIGURES E-3 THROUGH E-5
7. SHORT DASHES SHOW PERFORMANCE WITH UNMODIFIED SECOND-GENERATION PBDS; CURVE OBTAINED FROM USAAEFA REPORT 83-13
8. LONG DASHES SHOW PERFORMANCE WITH STANDARD BLADES; CURVE OBTAINED FROM USAAEFA REPORT 83-13

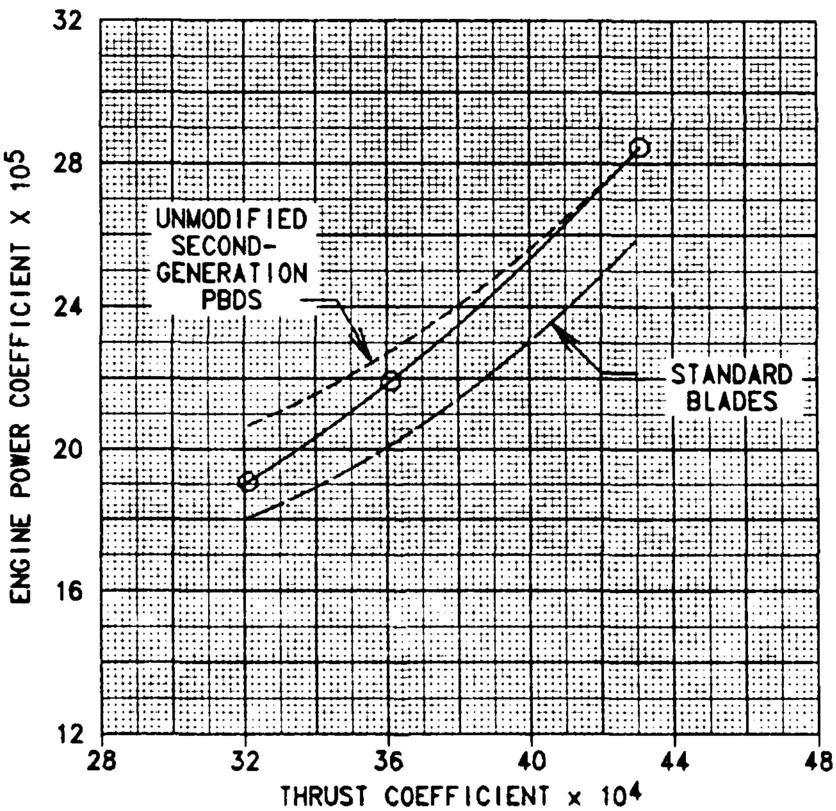

FIGURE E-13

LEVEL FLIGHT PERFORMANCE
JUH-1H USA S/N 70-16318
MODIFIED SECOND-GENERATION PNEUMATIC BOOT DEICING SYSTEM

AVG GROSS WEIGHT (LB)	AVG CG LOCATION LONG (FS)	AVG CG LOCATION LAT (BL)	AVG DENSITY ALTITUDE (FT)	AVG OAT (DEG C)	AVG REFERRED ROTOR SPEED (RPM)	AVG C_T $\times 10^4$	CONFIGURATION
7750	132.4	1.3 LT	8190	11.5	319.9	36.10	PBDS VENTED

NOTES: 1. AVERAGE ROTOR SPEED = 318 RPM
2. ZERO SIDESLIP

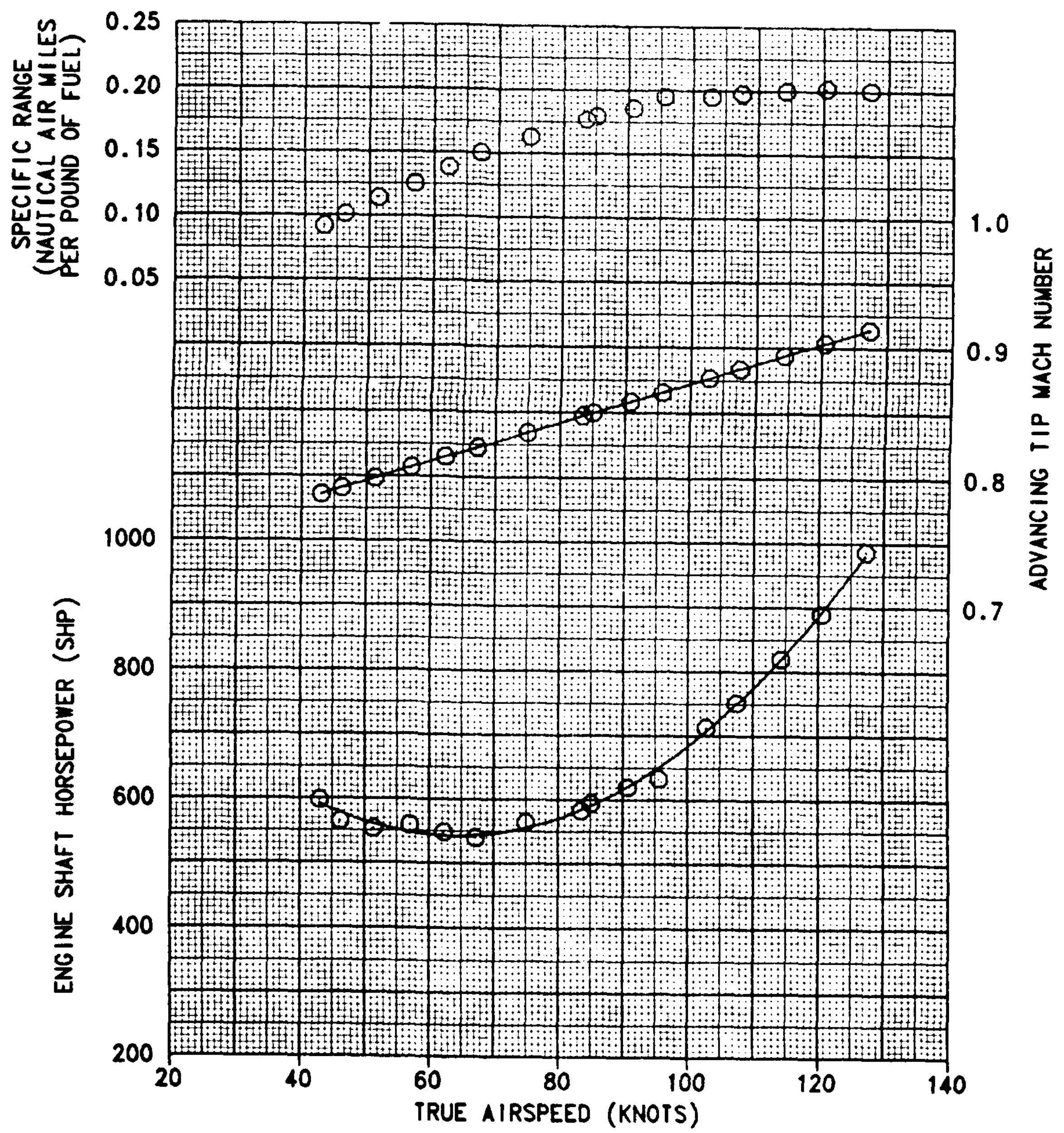

TABLE E-1

FLIGHT CONDITION		MAIN ROTOR BLADE CHORDWISE BENDING MOMENT Blade Station 192 (1000 in-lb) PBDS CONDITION						MAIN ROTOR PITCH LINK AXIAL LOAD (lb) PBDS CONDITION					
		Normal		Cycled		Vented		Normal		Cycled		Vented	
		steady	oscil	steady	oscil	steady	oscil	steady	oscil	steady	oscil	steady	oscil
IGE HOVER		-5.8	1.8	-5.1	1.8	-4.8	3.0	340.0	120.0	130.0	110.0	296.8	121.1
LOW-SPEED FLIGHT													
FORWARD	10 KTAS	-4.8	3.6	-4.2	4.9	-4.8	3.6	393.7	145.4	248.3	169.6	321.0	145.4
	20 KTAS	-6.6	7.3	-6.6	7.3	-5.4	7.3	272.6	218.0	103.0	218.0	190.0	270.0
	40 KTAS	-6.6	7.3	-6.6	7.3	NOT TESTED		210.0	200.0	80.0	240.0	NOT TESTED	
RIGHT	10 KTAS	-4.8	3.6	-4.2	5.5	-4.8	3.6	369.5	96.9	248.3	72.7	345.2	242.3
	20 KTAS	-6.6	12.1	-6.6	12.1	-5.4	10.9	296.8	193.8	151.4	193.8	190.0	210.0
LEFT	10 KTAS	-4.8	3.6	-4.2	6.1	-4.8	4.2	393.7	145.4	272.6	242.3	296.8	145.4
	20 KTAS	-5.4	7.3	-5.4	7.3	-5.4	5.3	248.3	242.3	6.1	387.6	100.0	390.0
REARWARD	10 KTAS	-5.4	9.7	-4.2	9.7	-5.4	6.1	417.9	290.7	224.1	363.4	296.8	290.7
	20 KTAS	-9.0	9.7	-9.0	9.7	-9.0	10.9	240.0	340.0	100.0	390.0	190.0	440.0
LEVEL FLIGHT (314 RPM)	50 KIAS	-5.4	4.2	-4.2	6.1	-4.8	4.6	296.8	266.5	30.3	363.4	151.4	266.5
	60 KIAS	-5.4	4.2	-4.8	5.5	-4.8	4.2	272.6	290.7	6.1	387.6	151.4	290.7
	70 KIAS	-5.4	4.2	-4.2	4.9	-5.4	3.6	296.8	315.0	103.0	436.1	199.9	363.4
	80 KIAS	-4.8	4.2	-3.6	6.7	-5.4	4.9	345.2	363.4	103.0	508.8	199.9	387.6
	90 KIAS	-4.8	4.2	-3.6	7.3	-4.8	5.5	369.5	508.8	248.3	605.7	199.9	460.3
	100 KIAS	-4.2	5.5	-1.8	12.1	-4.2	5.5	393.7	533.0	393.7	751.1	224.1	553.0
	110 KIAS	-3.6	7.3	NOT TESTED		-3.0	7.3	447.1	581.5	NOT TESTED		248.3	654.1
LEVEL FLIGHT (323 RPM)	50 KIAS	-8.4	4.9	-6.6	7.3	-6.0	4.6	224.1	242.3	6.1	315.0	127.2	193.8
	60 KIAS	-8.4	4.2	-6.6	4.9	-6.0	4.6	248.3	242.3	30.3	339.2	127.2	290.7
	70 KIAS	-7.8	3.6	-6.6	6.1	-6.0	4.2	248.3	290.7	30.3	363.4	127.2	315.0
	80 KIAS	-6.6	3.6	-6.0	5.5	-6.0	3.6	296.8	315.0	127.2	436.1	151.4	387.6
	90 KIAS	-6.0	4.2	-5.4	4.2	-6.0	4.2	369.5	484.5	199.9	557.2	151.4	460.3
	100 KIAS	-5.4	4.9	-3.6	6.1	-5.4	4.9	393.7	581.5	248.3	728.6	199.9	557.2
	110 KIAS	-4.2	4.9	NOT TESTED		-4.2	4.9	345.2	581.5	NOT TESTED		224.1	581.5
CLIMB													
45 PSI TORQUE,	60 KIAS	-3.0	4.9	-1.8	6.1	-3.0	5.5	442.2	411.9	151.4	460.3	321.0	363.4
45 PSI TORQUE,	90 KIAS	-3.6	6.1	-3.0	7.3	-3.0	7.3	417.9	533.0	199.9	605.7	248.3	557.2
DESCENT													
8 PSI TORQUE,	60 KIAS	-9.7	3.6	-9.7	3.6	-10.3	3.0	6.1	339.2	-139.3	387.6	-236.2	266.5
10 PSI TORQUE,	90 KIAS	-10.9	4.2	-10.9	3.6	-10.3	3.6	54.5	339.2	-139.3	533.0	-163.5	363.4
AUTOROTATION	60 KIAS	NOT TESTED				-12.1	3.6	NOT TESTED				-236.2	266.5
RIGHT TURN 30 DEG,	90 KIAS	-6.0	4.6	-4.2	7.9	-5.4	4.9	345.2	508.8	151.4	726.8	151.4	557.2
LEFT TURN 30 DEG,	90 KIAS	-6.0	4.2	-5.4	5.5	-6.0	4.2	345.2	508.8	199.9	557.2	175.6	484.5
ENGINE FAILURE	60 KIAS	NOT TESTED				-9.7	3.0	NOT TESTED				-263.2	266.5
	90 KIAS	NOT TESTED				-10.9	3.6	NOT TESTED				-263.2	363.4

NOTES:
Average aircraft gross weight was 7600 lb, average aircraft longitudinal cg was 136.5, pressure altitude was 6000 ft for all tests except hover and low-speed flight, for which it was 2000 ft, and main rotor speed was 323 rpm except as noted.
Main rotor pitch link steady-state oscillatory endurance limit = +- 750 lb

TABLE E-2

FLIGHT CONDITION		MAIN ROTOR HUB CHORDWISE BENDING MOMENT Blade Station 5.5 (1000 in-lb) PBDS CONDITION						MAIN ROTOR HUB BEAMWISE BENDING MOMENT Blade Station 5.5 (1000 in-lb) PBDS CONDITION					
		Normal		Cycled		Vented		Normal		Cycled		Vented	
		steady	oscil	steady	oscil	steady	oscil	steady	oscil	steady	oscil	steady	oscil
IGE HOVER		70.0	13.0	80.0	11.0	31.1	13.3	-50.0	4.4	-47.1	5.9	-129.8	5.9
LOW-SPEED FLIGHT													
FORWARD	10 KTAS	35.3	21.3	32.4	29.3	31.1	21.3	-132.8	11.8	-123.9	16.3	-129.8	8.9
	20 KTAS	78.2	42.6	75.6	53.3	60.0	53.3	-50.0	11.8	-45.6	11.8	-47.1	14.8
	40 KTAS	54.2	42.6	64.9	42.6	NOT TESTED		-53.0	20.7	-50.0	20.7	NOT TESTED	
RIGHT	10 KTAS	34.3	16.0	33.1	21.3	36.2	24.0	-131.3	8.9	-129.8	17.7	-128.3	8.9
	20 KTAS	64.9	53.3	128.8	53.3	59.6	58.6	-45.6	17.7	-44.1	17.7	-50.0	20.7
LEFT	10 KTAS	31.2	26.6	31.2	45.3	33.8	16.0	-129.8	8.9	-123.9	14.8	-129.8	10.3
	20 KTAS	70.2	42.6	131.5	42.6	67.6	42.6	-44.1	11.8	-41.2	11.8	-47.1	14.8
REARWARD	10 KTAS	35.6	26.6	35.2	26.6	34.7	32.0	-131.3	8.9	-126.8	22.2	-129.8	14.8
	20 KTAS	56.6	48.0	70.2	53.3	56.6	48.0	-53.0	17.7	-47.1	17.7	-50.0	17.7
LEVEL FLIGHT (314 RPM)	50 KIAS	43.6	34.6	62.2	45.3	46.2	37.3	-27.9	11.8	-22.0	17.7	-36.7	13.3
	60 KIAS	43.6	34.6	62.2	48.0	48.9	34.6	-29.3	10.3	-29.5	16.3	-32.3	13.3
	70 KIAS	48.4	34.6	67.6	42.6	51.6	34.6	-26.4	10.3	-22.0	19.2	-33.8	8.9
	80 KIAS	54.2	42.6	72.9	58.6	56.9	37.3	-29.3	13.3	-23.4	17.7	-36.7	11.8
	90 KIAS	64.9	48.0	83.5	69.3	70.2	42.6	-24.9	17.7	-20.5	22.2	-35.3	13.3
	100 KIAS	70.2	50.6	91.5	93.3	75.6	50.6	-27.9	22.0	-23.4	32.5	-26.4	23.6
	110 KIAS	80.9	58.6	NOT TESTED		86.2	58.6	-24.9	23.6	NOT TESTED		-29.3	23.6
LEVEL FLIGHT (323 RPM)	50 KIAS	51.6	16.0	75.6	32.0	48.9	34.6	-47.1	16.3	-35.3	11.8	-45.6	14.8
	60 KIAS	48.9	26.6	70.2	32.0	48.9	32.0	-44.1	13.3	-41.2	10.3	-41.2	13.3
	70 KIAS	48.9	32.0	70.2	42.6	46.2	32.0	-50.0	10.3	-41.2	11.8	-45.6	11.8
	80 KIAS	56.9	32.0	75.6	48.0	54.2	34.6	-47.1	14.8	-41.2	14.8	-47.1	10.3
	90 KIAS	62.2	40.0	78.2	45.3	67.6	37.3	-32.3	14.8	-29.3	17.7	-42.6	16.3
	100 KIAS	75.6	42.6	88.9	56.0	72.9	37.3	-32.3	22.2	-20.5	22.2	-45.6	19.2
	110 KIAS	78.2	42.6	NOT TESTED		88.9	42.9	-38.2	22.2	NOT TESTED		-42.6	23.6
CLIMB													
45 PSI TORQUE,	60 KIAS	91.5	48.0	104.9	48.0	102.2	42.6	-32.2	8.9	-33.8	11.8	-44.1	7.4
45 PSI TORQUE,	90 KIAS	102.2	53.3	107.5	64.0	102.2	50.6	-26.4	17.7	-29.3	19.2	-38.2	19.2
DESCENT													
8 PSI TORQUE,	60 KIAS	11.6	26.6	22.3	26.6	56.9	26.6	-44.1	14.8	-42.6	16.3	-57.4	14.8
10 PSI TORQUE,	90 KIAS	11.6	34.6	27.6	26.6	14.3	34.6	-42.6	13.3	-41.2	17.7	-53.0	16.3
AUTOROTATION	60 KIAS	NOT TESTED				-1.7	29.3	NOT TESTED				-50.0	11.8
RIGHT TURN													
30 DEG,	90 KIAS	59.6	40.0	78.2	64.0	59.6	40.0	-23.4	17.7	-13.1	20.7	-24.9	19.2
LEFT TURN													
30 DEG,	90 KIAS	62.2	42.6	78.2	48.0	64.9	42.6	-24.9	18.5	-35.3	16.3	-38.2	17.7
ENGINE FAILURE	60 KIAS	NOT TESTED				-4.4	26.6	NOT TESTED				-42.6	16.3
	90 KIAS	NOT TESTED				-7.1	34.6	NOT TESTED				-38.2	14.8

NOTES:
Average aircraft gross weight was 7600 lb, average aircraft longitudinal cg was 136.5, pressure altitude was 6000 ft for all tests except hover and low-speed flight, for which it was 2000 ft, and main rotor speed was 323 rpm except as noted.

TABLE E-3

FLIGHT CONDITION		FORWARD/AFT CYCLIC BOOST ACTUATOR LOAD (lb) PBDS CONDITION Normal steady	Normal oscil	Cycled steady	Cycled oscil	Vented steady	Vented oscil	LATERAL CYCLIC BOOST ACTUATOR LOAD (lb) PBDS CONDITION Normal steady	Normal oscil	Cycled steady	Cycled oscil	Vented steady	Vented oscil
IGE HOVER		48.8	240.0	48.8	240.0	-15.2	208.0	28.6	254.6	28.6	254.6	28.6	190.9
LOW-SPEED FLIGHT													
FORWARD	10 KTAS	-15.2	256.0	64.0	256.0	16.8	256.0	60.5	206.9	92.3	254.6	44.6	222.8
	20 KTAS	80.8	320.0	144.8	320.0	112.8	384.0	28.6	254.6	28.6	254.6	11.7	62.5
	40 KTAS	48.8	352.0	48.8	352.0	NOT	TESTED	-98.6	413.7	-98.6	413.7	NOT	TESTED
RIGHT	10 KTAS	-47.2	224.0	16.8	192.0	-31.2	224.0	28.6	238.7	28.6	238.7	124.1	238.7
	20 KTAS	-111.2	288.0	-111.2	288.0	-95.2	320.0	-130.5	254.6	-162.3	254.6	-194.1	286.4
LEFT	10 KTAS	-47.2	256.0	-15.2	256.0	-47.2	160.0	124.1	222.8	124.1	222.8	-3.2	190.9
	20 KTAS	16.8	288.0	-95.2	256.0	-143.2	320.0	92.3	286.4	124.1	381.9	92.3	429.6
REVERSE	10 KTAS	-175.2	224.0	-175.2	288.0	-111.2	256.0	-3.2	286.4	-35.0	350.1	-35.0	286.4
	20 KTAS	-207.2	288.0	-207.2	320.0	-207.2	320.0	-98.6	413.7	-98.6	413.7	-98.6	445.5
LEVEL FLIGHT (314 RPM)	50 KIAS	176.8	256.0	208.8	304.0	192.8	240.0	12.7	318.2	60.5	334.2	44.6	302.3
	60 KIAS	176.8	264.0	208.8	304.0	192.8	256.0	-19.1	334.2	44.6	334.2	-3.2	318.2
	70 KIAS	224.8	304.0	208.8	352.0	192.8	304.0	-3.2	318.2	28.6	366.0	12.7	318.2
	80 KIAS	192.8	336.0	304.8	416.0	240.8	369.0	-19.1	318.2	92.3	461.4	12.7	302.3
	90 KIAS	304.8	448.0	400.8	496.0	272.8	400.0	-19.1	206.9	76.4	445.5	44.6	286.4
	100 KIAS	240.8	512.0	432.8	512.0	288.8	496.0	-19.1	238.7	44.6	413.7	44.6	222.8
	110 KIAS	240.8	576.0	NOT	TESTED	272.8	528.0	-50.9	270.5	NOT	TESTED	28.6	302.3
LEVEL FLIGHT (323 RPM)	50 KIAS	208.8	288.0	144.8	320.0	208.8	288.0	-50.9	286.4	28.6	350.1	44.6	302.3
	60 KIAS	144.8	160.0	176.8	320.0	240.8	320.0	-50.9	313.2	60.5	334.2	44.6	318.2
	70 KIAS	176.8	320.0	208.8	352.0	224.8	336.0	-66.8	350.1	44.6	397.8	44.6	302.3
	80 KIAS	176.8	384.0	240.8	416.0	256.8	368.0	-35.0	254.6	-3.2	318.2	76.4	254.6
	90 KIAS	224.8	448.0	304.8	464.0	256.8	416.0	-28.6	222.8	108.2	302.3	60.5	238.7
	100 KIAS	192.8	544.0	368.8	576.0	320.8	496.0	-35.0	254.6	92.3	270.5	60.5	206.9
	110 KIAS	240.8	528.0	NOT	TESTED	288.8	528.0	-35.0	238.7	NOT	TESTED	60.5	206.9
CLIMB													
45 PSI TORQUE,	60 KIAS	208.8	384.0	208.8	400.0	224.8	368.0	12.7	257.6	60.5	302.3	12.7	270.5
45 PSI TORQUE,	90 KIAS	208.8	496.0	304.8	496.0	240.8	480.0	-35.0	270.5	92.3	238.7	-3.2	254.6
DESCENT													
8 PSI TORQUE,	60 KIAS	112.8	336.0	128.8	320.0	80.8	288.0	44.6	397.8	60.5	429.6	28.6	381.9
10 PSI TORQUE,	90 KIAS	176.8	352.0	240.8	416.0	176.8	304.0	60.5	334.2	92.3	413.7	44.6	334.2
AUTOROTATION	60 KIAS		NOT	TESTED		96.8	288.0		NOT	TESTED		98.6	397.8
RIGHT TURN 30 DEG,	90 KIAS	224.8	496.0	400.8	528.0	240.8	448.0	44.6	222.8	76.4	334.2	44.6	222.8
LEFT TURN 30 DEG,	90 KIAS	208.8	448.0	352.8	464.0	224.8	432.0	44.6	222.8	42.3	254.6	44.6	190.9
ENGINE FAILURE	60 KIAS		NOT	TESTED		128.8	320.0		NOT	TESTED		28.6	413.7
	90 KIAS		NOT	TESTED		176.8	320.0		NOT	TESTED		60.5	445.5

NOTES:
Average aircraft gross weight was 7600 lb, average aircraft longitudinal cg was 136.5, pressure altitude was 6000 ft for all tests except hover and low-speed flight, for which it was 2000 ft, and main rotor speed was 323 rpm except as noted.

TABLE E-4

COLLECTIVE BOOST ACTUATOR LOAD (lb)

PBDS CONDITION

FLIGHT CONDITION		Normal steady	Normal oscil	Cycled steady	Cycled oscil	Vented steady	Vented oscil
IGE HOVER		-113.3	46.9	11.7	46.9	-19.6	15.6
LOW-SPEED FLIGHT							
FORWARD	10 KTAS	-82.1	31.3	43.0	46.9	-19.6	31.3
	20 KTAS	-66.4	43.0	-66.4	62.5	11.7	62.5
	40 KTAS	-3.9	62.5	105.5	46.9	NOT	TESTED
RIGHT	10 KTAS	-82.1	31.3	43.0	46.9	-19.6	46.9
	20 KTAS	-50.8	31.3	58.6	31.3	11.7	46.9
LEFT	10 KTAS	-82.1	46.9	43.0	62.5	-19.6	31.3
	20 KTAS	-66.4	62.5	74.2	62.5	11.7	93.8
REVERSE	10 KTAS	-82.1	46.9	43.0	62.5	-19.6	46.9
	20 KTAS	-82.1	78.1	43.0	109.4	-19.6	109.4
LEVEL FLIGHT (314 RPM)	50 KIAS	-19.6	54.7	82.0	31.3	50.8	39.1
	60 KIAS	-11.7	62.5	82.0	54.7	58.6	46.9
	70 KIAS	-35.2	70.3	58.6	78.1	27.3	78.1
	80 KIAS	-50.8	70.3	58.6	78.1	27.3	93.8
	90 KIAS	-89.9	93.8	11.7	109.4	-3.9	117.2
	100 KIAS	-129.0	132.9	-50.8	171.9	-35.2	132.9
	110 KIAS	-144.6	132.9	NOT	TESTED	-97.7	156.3
LEVEL FLIGHT (323 RPM)	50 KIAS	11.7	46.9	136.7	46.9	58.6	46.9
	60 KIAS	11.7	46.9	121.1	46.9	74.2	46.9
	70 KIAS	-50.8	93.8	74.2	93.8	58.6	54.7
	80 KIAS	-82.1	78.1	43.0	78.1	43.0	62.5
	90 KIAS	-66.4	46.9	43.0	70.3	11.7	70.3
	100 KIAS	-129.0	86.0	-35.2	101.6	-19.6	86.0
	110 KIAS	-129.0	78.1	NOT	TESTED	-50.8	117.2
CLIMB							
45 PSI TORQUE,	60 KIAS	-175.8	78.1	-35.2	93.8	-113.3	78.1
45 PSI TORQUE,	90 KIAS	-191.5	93.8	-43.0	109.4	-129.0	109.4
DESCENT							
8 PSI TORQUE,	60 KIAS	183.6	78.1	308.7	70.3	371.2	54.7
10 PSI TORQUE,	90 KIAS	160.2	62.5	277.4	70.3	293.0	54.7
AUTOROTATION	60 KIAS		NOT	TESTED		324.3	62.5
RIGHT TURN 30 DEG,	90 KIAS	-66.4	62.5	74.2	78.1	27.3	62.5
LEFT TURN 30 DEG,	90 KIAS	-66.4	54.7	43.0	70.3	27.3	62.5
ENGINE FAILURE	60 KIAS		NOT	TESTED		371.2	96.9
	90 KIAS		NOT	TESTED		255.6	46.9

NOTES:
Average aircraft gross weight was 7600 lb, average aircraft longitudinal cg was 136.5, pressure altitude was 6000 ft for all tests except hover and low-speed flight, for which it was 2000 ft, and main rotor speed was 323 rpm except as noted.

DISTRIBUTION

HQDA (DALO-AV)	1
HQDA (DALO-FDQ)	1
HQDA (DAMO-HRS)	1
HQDA (SARD-PPM-T)	1
HQDA (SARD-RA)	1
HQDA (SARD-WSA)	1
US Army Material Command (AMCDE-SA, AMCDE-P, AMCQA-SA, AMCQA-ST)	4
US Training and Doctrine Command (ATCD-T, ATCD-B)	2
US Army Aviation Systems Command (AMSAV-8, AMSAV-Q, AMSAV-MC, AMSAV-ME, AMSAV-L, AMSAV-N, AMSAV-GTD)	8
US Army Test and Evaluation Command (AMSTE-TE-V, AMSTE-TE-O)	2
US Army Logistics Evaluation Agency (DALO-LEI)	1
US Army Materiel Systems Analysis Agency (AMXSY-RV, AMXSY-MP)	8
US Army Operational Test and Evaluation Agency (CSTE-AVSD-E)	2
US Army Armor School (ATSB-CD-TE)	1
US Army Aviation Center (ATZQ-D-T, ATZQ-CDC-C, ATZQ-TSM-A, ATZQ-TSM-S, ATZQ-TSM-LH)	5
US Army Combined Arms Center (ATZL-TIE)	1
US Army Safety Center (PESC-SPA, PESC-SE)	2
US Army Cost and Economic Analysis Center (CACC-AM)	1
US Army Aviation Research and Technology Activity (AVSCOM) NASA/Ames Research Center (SAVRT-R, SAVRT-M (Library)	3

US Army Aviation Research and Technology Activity (AVSCOM)	2
Aviation Applied Technology Directorate (SAVRT-TY-DRD, SAVRT-TY-TSC (Tech Library)	
US Army Aviation Research and Technology Activity (AVSCOM)	1
Aeroflightdynamics Directorate (SAVRT-AF-D)	
US Army Aviation Research and Technology Activity (AVSCOM	1
Propulsion Directorate (SAVRT-PN-D)	
Defense Technical Information Center (FDAC)	2
US Military Academy, Department of Mechanics (Aero Group Director)	1
ASD/AFXT, ASD/ENF	2
US Army Aviation Development Test Activity (STEBG-CT)	2
Assistant Technical Director for Projects, Code: CT-24 (Mr. Joseph Dunn)	2
6520 Test Group (ENML)	1
Commander, Naval Air Systems Command (AIR 5115B, AIR 5301)	3
Defense Intelligence Agency (DIA-DT-2D)	1
School of Aerospace Engineering (Dr. Daniel P. Schrage)	1
Headquarters United States Army Aviation Center and Fort Rucker (ATZQ-ESO-L)	1
US Army Aviation Systems Command (AMSAV-EA)	1
US Army Aviation Systems Command (AMSAV-ECH)	1
US Army Aviation Systems Command (AMSAV-UH)	1
Director, Aviation Applied Technology Directorate, AVSCOM (SAVRT-TY-ASR, Harvey Young)	2